Rev Bras Anestesiol. 2018;68(1):1–32

Sociedade Brasileira de Anestesiologia

REVISTA BRASILEIRA DE ANESTESIOLOGIA

Publicação Oficial da Sociedade Brasileira de Anestesiologia
www.sba.com.br

SPECIAL ARTICLE

Consensus on Perioperative Transesophageal Echocardiography of the Brazilian Society of Anesthesiology and the Department of Cardiovascular Image of the Brazilian Society of Cardiology

Marcello Fonseca Salgado-Filho[a,b,*], Samira Saady Morhy[c,d], Henrique Doria de Vasconcelos[a,e,f], Eric Benedet Lineburger[a,g], Fabio de Vasconcelos Papa[a,h], Eduardo Souza Leal Botelho[a,i,j], Marcelo Ramalho Fernandes[a,k,l], Maurício Daher[a,m], David Le Bihan[c,n,o,p], Chiara Scaglioni Tessmer Gatto[a,q,r], Cláudio Henrique Fischer[c,d,s], Alexander Alves da Silva[a,t], Carlos Galhardo Júnior[a,i], Carolina Baeta Neves[a,n,s], Alexandre Fernandes[a,i,j], Marcelo Luiz Campos Vieira[c,d,q,r]

[a] *Núcleo Vida – Ecocardiografia Transesofágica Intraoperatória da Sociedade Brasileira de Anestesiologia (ETTI/SBA), Rio de Janeiro, RJ, Brazil*
[b] *Universidade Federal de Juiz de Fora (UFJF), Juiz de Fora, MG, Brazil*
[c] *Departamento de Imagem Cardiovascular da Sociedade Brasileira de Cardiologia (DIC/SBC), São Paulo, SP, Brazil*
[d] *Hospital Israelita Albert Einstein, São Paulo, SP, Brazil*
[e] *Universidade Federal do Vale da São Francisco (Univasf), Petrolina, PE, Brazil*
[f] *Jonhs Hopkins University, Baltimore, USA*
[g] *Hospital São José, Criciúma, SC, Brazil*
[h] *Takaoka Anestesia, São Paulo, SP, Brazil*
[i] *Instituto Nacional de Cardiologia (INC), Rio de Janeiro, RJ, Brazil*
[j] *Universidade do Estado do Rio de Janeiro (UERJ), Rio de Janeiro, RJ, Brazil*
[k] *Hospital Pró-Cardíaco, Rio de Janeiro, RJ, Brazil*
[l] *Hospital Copa Star, Rio de Janeiro, RJ, Brazil*
[m] *Instituto de Cardiologia do Distrito Federal, Brasília, DF, Brazil*
[n] *Instituto Dante Pazzanese de Cardiologia, São Paulo, SP, Brazil*
[o] *Hospital do Rim e Hipertensão, São Paulo, SP, Brazil*
[p] *Grupo Dasa, São Paulo, SP, Brazil*
[q] *Instituto do Coração (Incor), São Paulo, SP, Brazil*

* Corresponding author.
E-mail: mfonsecasalgado@hotmail.com (M.F. Salgado-Filho).

https://doi.org/10.1016/j.bjane.2017.09.001

[r] *Faculdade de Medicina da Universidade de São Paulo (FMUSP), São Paulo, SP, Brazil*
[s] *Universidade Federal de São Paulo (Unifesp), São Paulo, SP, Brazil*
[t] *São Paulo Serviços Médicos de Anestesia (SMA), São Paulo, SP, Brazil*

Received 20 June 2017; accepted 17 July 2017
Available online 16 October 2017

KEYWORDS
Echocardiography;
Transesophageal;
Perioperative

Abstract Through the Life Cycle of Intraoperative Transesophageal Echocardiography (ETTI/SBA) the Brazilian Society of Anesthesiology, together with the Department of Cardiovascular Image of the Brazilian Society of Cardiology (DIC/SBC), created a task force to standardize the use of intraoperative transesophageal echocardiography by Brazilian anesthesiologists and echocardiographers based on scientific evidence from the Society of Cardiovascular Anesthesiologists/American Society of Echocardiography (SCA/ASE) and the Brazilian Society of Cardiology.

PALAVRAS-CHAVE
Ecocardiografia;
Transesofágico;
Perioperatório

Consenso sobre Ecocardiografia Transesofágica Perioperatória da Sociedade Brasileira de Anestesiologia e do Departamento de Imagem Cardiovascular da Sociedade Brasileira de Cardiologia

Resumo A Sociedade Brasileira de Anestesiologia, pelo Núcleo Vida de Ecocardiografia Transesofágica Intraoperatória (ETTI/SBA) juntamente com o Departamento de Imagem Cardiovascular da Sociedade Brasileira de Cardiologia (DIC/SBC), fez uma força-tarefa para normatizar a feitura da ecocardiografia transesofágica intraoperatória para os anestesiologistas e ecocardiografistas brasileiros com base nas evidências científicas da Sociedade dos Anestesiologistas Cardiovasculares/Sociedade Americana de Ecocardiografia (SCA/ASE) e da Sociedade Brasileira de Cardiologia.

Introduction

Since its introduction in clinical practice in the late 1980s, transesophageal echocardiogram (TEE) has become one of the main diagnostic modalities in cardiology, as it guides anesthetic/surgical procedures and reduces morbidity and mortality in cardiac surgeries.[1] Due to the great proximity of the esophagus to the heart, to the absence of bones or lung tissue, and the use of high frequency transducers, it is possible to obtain high quality images.[1]

The first guideline on perioperative TEE was published in 1999 by the Society of Cardiovascular Anesthesiologists/American Society of Echocardiography (SCA/ASE), which defined the nomenclature and the 20 cross-sections for basic TEE.[2] In Brazil, we have the Brazilian Society of Cardiology (SBC) guidelines on the use of TEE.[3] The levels of evidence and indications for using TEE in cardiac and non-cardiac surgeries are shown in Table 1.

The SCA/ASE and SBC guidelines define professionals qualified to use echocardiography as a diagnostic method or as hemodynamic monitoring according to their basic and advanced knowledge criteria.[1,3] In Brazil, the area of perioperative echocardiography activity is being defined by the Brazilian Society of Anesthesiology (SBA) and SBC. As a first step in the standardization of this qualification and in order to promote continuing education to its members, in the last five years the SBA has taught the course of intraoperative echocardiography (ETI/SBA), divided into two modules, basic (Module I) and advanced (Module II).[4]

Thus, the SBA and DIC/SBC consensus on intraoperative TEE aims to standardize intraoperative echocardiography for Brazilian anesthesiologists and echocardiographers based on the scientific evidence of ASE/SCA and SBC.

Equipment

TEE probe was developed to improve images for which the transthoracic technique had limitations, such as for obese and emphysematous patients and those with thoracic anomalies.[1] The TEE ultrasound wave passes only through the esophagus and pericardium to form the heart images. In this way, images with higher resolution and greater number of anatomical sections are obtained (Fig. 1). In addition,

Table 1 Level of evidence – intraoperative transesophageal echocardiography.

Recommendation	Class
Severe, acute, and persistent hemodynamic disorders, with doubtful ventricular function, irresponsive to treatment	I
Valve lesion repair or surgical replacement, aortic disease, and hypertrophic cardiomyopathy	I
Ventricular aneurysm, cardiac tumor removal, intracardiac thrombectomy, and pulmonary embolectomy	I
Congenital heart disease surgery with cardiopulmonary bypass	I
Placement of intracardiac devices	I
Assessment of localized or posterior pericardial effusion	I
Assessment of transcatheter procedures (interatrial communication closure, atrial appendage occlusion, transcatheter valve procedures)	I
Myocardial function assessment after myocardial revascularization with or without cardiopulmonary bypass	IIa
Large non-cardiac surgery in high-risk patients	IIa

the TEE transducer may be attached to a specific part of the esophagus or stomach, which allows a more detailed analysis of the cardiac anatomy.[1,5] The current TEE transducers operate at a frequency of 3.5–7 MHz, reaching up to 20 MHz.[5]

Most adult TEE probes have two knobs on the handle. One for anteflex and retroflex movements and the other for lateral movement, clockwise and counterclockwise.[1] Multiplane transducers have ultrasonic beam angle control, which can vary from zero degrees to 180°. All these controls, associated with the probe removal and introduction into the esophagus, allow the visualization of several echocardiographic cross-sections (Fig. 2).[1,6]

Adult TEE probe measures about 100 cm and the diameter varies from 9 to 12 mm, 1 to 2 mm thicker at the tip. For using an adult TEE probe, the patient should weigh at least 20 kg.[7]

Complications

TEE-related complications may be separated into two groups: (1) Direct esophageal, stomach and/or airway trauma; (2) TEE indirect effects (Table 2).[1]

In group 1, complications include esophageal bleeding, burning, dysphagia, and laryngeal discomfort.[6] Most of these complications occur during the catheter passage. In patients undergoing cardiopulmonary bypass, the probe passage should occur prior to heparinization and withdrawal should occur only after reversal with protamine and with activated clotting time (ACT) less than 120 s.[1]

In a study of 10,000 TEE exams, there was one case of hypopharyngeal perforation (0.01%), two cases of cervical esophageal perforation (0.02%), and no case of gastric perforation. The incidence of morbidity and mortality is 0.2% and zero, respectively.[8]

The most common complications associated with the intraoperative use of TEE are: odynophagia (0.1%), dental injury (0.03%), orotracheal tube misplacement (0.03%), upper gastrointestinal bleeding (0.03%), and bacteremia (0–17%). Although the incidence of bacteremia is high, there is no correlation with the development of infectious endocarditis.[8]

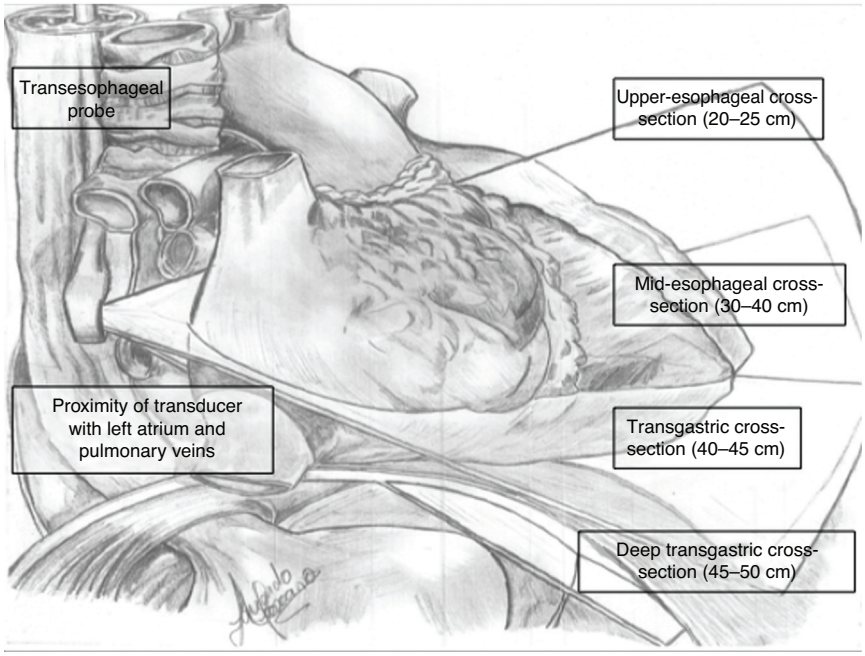

Figure 1 Anatomical relationships for transesophageal probe, esophagus, and heart.

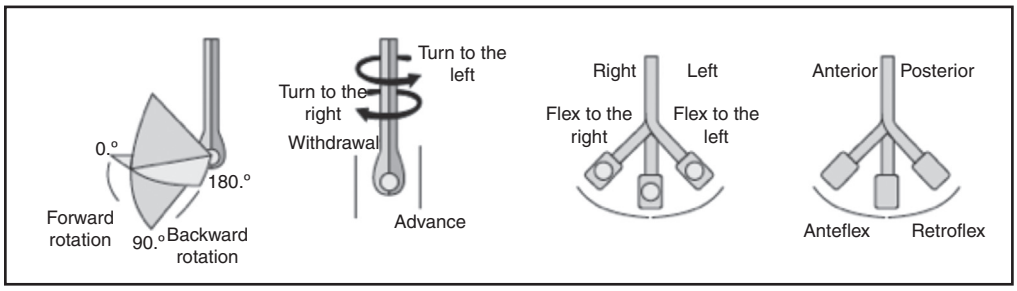

Figure 2 Probe and transducer handling movements to acquire echocardiographic images. Adapted from Galhardo et al.[6]

Table 2 Transesophageal echocardiography complications.

Airway and esophagus direct trauma
Esophageal bleeding
Esophageal burn
Dysphagia
Bacteremia
Vocal cord paralysis
Indirect effects
Hemodynamic and pulmonary changes
Inadvertent airway management
Distraction during patient care

In group 2, we have complications indirectly related to TEE, which include: hemodynamic, pulmonary changes, airway manipulations, and distraction during patient care.[8] It is important to leave all anesthesia workstation and monitor alarms turned on, as the TEE device may be positioned in a way that makes it difficult to see all the monitors at once. Furthermore, during examination, the examiner may become inattentive with the patient and attempt to do some echocardiographic imaging or make a diagnosis. Initially, echocardiographic examination with a second anesthesiologist at site is important so that, while one anesthesiologist performs the echocardiographic exam, the other helps in the intensive control of the patient.[1,9]

Probe passing technique

Probe introduction should be performed with the patient under anesthesia after tracheal intubation.[1] Probe should be lubricated with proper TEE gel (usually lidocaine gel or intimate lubricant), and the stomach may be previously emptied to enhance the images.[1]

Probe passing is often a challenge. The technique consists of proper lubrication of the probe, passing it through the posterior oropharynx and elevating the mandible with the left hand. Passing it through the upper esophageal sphincter is the procedure critical time in which the most serious complications may occur. The probe should progress toward the esophagus without resistance.[6] In case of resistance, this usually occurs because the probe's tip is lodged in the pyriform sinus, epiglottic vallecula, posterior part of the tongue, or esophageal diverticula. The probe should never be forced against resistance, as it may lead to complications such as perforation and bleeding.[1]

Another technique that can be used is the probe introduction with the help of a laryngoscope. In this case, care should be taken with the hemodynamic stimulus triggered by a second laryngoscopy.[1]

The TEE examination allows intra- and extracardiac anatomical analysis of the great vessels at the base, analysis of congenital heart defects, and qualitative and quantitative analysis of Doppler flow.[1,3] A complete intraoperative examination not only characterizes the patient's hemodynamic profile but may lead to changes in the surgical approach in up to 25% of the exams, in which changes such as the presence of a patent foramen ovale (PFO), left atrial (LA) thrombi, or atheroma plaques in the ascending aorta (Asc Ao).[8]

The examinations must be recorded on a digital media for further analysis and medical report. Thus, it is possible to analyze the patient's evolution both intraoperatively and postoperatively.[6]

Management of TEE probe

The correct use of the multiplane TEE probe functions provides adequate acquisition of cardiac images during intraoperative examination. In addition, its proper handling reduces the incidence of stomach and esophageal complications.

Moving the probe in the caudal and cranial direction produces changes in the images in the inferior and superior directions of the heart, respectively (high esophagus: about 20–25 cm; medium esophagus: about 30–40 cm; transgastric (TG): about 40–45 cm; deep TG: about 45–50 cm). Changes to the right or left of the heart can be obtained by moving the probe clockwise or counterclockwise. The best alignment of the images can be obtained with the anterior or posterior movement of the probe, using anteflexion or retroflexion with the help of the larger probe handle.[1] Multiplane TEE provides fine adjustments in the inclination angle of the image plane and consequently allows for more precise anatomical analysis. The angle may range from 0° to 180° (Fig. 2).[1]

Comprehensive echocardiographic examination

The technique description for performing the comprehensive transesophageal echocardiographic examination will

follow the ASE/ACS model.[1,2] The nomenclature of the mitral valve (MV) cusps will follow the classification of Carpentier et al.[10] The cross-sectional images established for this complete analysis are as follows.

Mid-esophageal five-chamber cross-section

Advance the probe up to 30 cm from the incisors in the mid-esophagus. Rotate the transducer angle up to 10° and look for the left ventricular outflow tract (LVOT) and aortic valve (AV) and flex the probe anteriorly. It is termed five chambers because we visualize the LA, right atrium (RA), left ventricle (LV), right ventricle (RV), and LVOT with part of the AV. The evaluation of regional LV function is impaired by the apex shortening (Fig. 3A).

Mid-esophageal four-chamber cross-section

Advance the probe from the previous position (five-chamber) up to 30–35 cm. We can describe the LV, RV, LA, RA, interatrial septum (IAS), MV, and tricuspid valve (TV). The true (not shortened) apex may be exposed by retroflexing the probe. It is one of the most used views for diagnosis (Fig. 3B).

Mid-esophageal mitral commissural cross-section

From the previous position (four-chamber), rotate the probe up to 45–60°. The MV has a typical appearance in this image (segments P_1–A_2–P_3), the section passes through the MV commissural axis. Papillary muscles and *chordae tendineae* are identified. Small manipulations of the probe in this image may provide anatomical details and a more complete analysis of the MV (Fig. 3C).

Mid-esophageal two-chamber cross-section

From the commissural view, rotate the angle between 60° and 90°. LA, left atrial appendage (LAA), LV, and MV are identified. The anterior and inferior walls are exposed and both ventricular and mitral valve function can be evaluated. Coronary venous sinus (CS) is seen on the short axis, just above the LV basal inferior wall (Fig. 3D).

Mid-esophageal long axis cross-section

In the two-chamber window, rotate the angle to 120°. LA, LV, LVOT, AV, proximal Asc Ao, CS, and MV (P_2 and A_2 segments) are visualized. Adjustments are made to maximize and accurately measure the LVOT diameter. The LV anteroseptal and inferolateral movements can be investigated (Fig. 4A).

Mid-esophageal aortic valve long-axis cross-section

The probe is retracted a few centimeters from the position of the long axis in the mid-esophagus. Maintaining an angle of 120–140°, the LVOT, AV, and proximal Asc Ao are aligned and, from this point, AV can be evaluated and the sinotubular and annular diameters of Ao measured. Finding protruding atherosclerotic plaques is also a utility of this window.

Mid-esophageal ascending aorta long axis cross-section

From the AV long axis view, the probe is removed, turned counterclockwise (90–110°). The walls of Asc Ao are inspected at various depths depending on the pathology. Dissection and graft sutures are examples of evaluations in this window (Fig. 4B). The Asc Ao distal portion and the proximal aortic arch are not usually visualized by this technique; they require complementation with ultrasound-epiaortic guidance for artery cannulation (Fig. 4C).

Upper esophageal ascending aorta short axis cross-section

From the AV long axis view (120–140°), the probe is withdrawn and, with 90° counterclockwise rotation, the images of Asc Ao short axis and superior vena cava (SVC) are obtained. The main pulmonary artery can be seen with bifurcation (probe rotation to the left) and the right pulmonary artery branch can be seen to a large extent (probe rotation to the right). It is a good window to check pulmonary artery catheter placement (Fig. 4D).

Mid-esophageal right pulmonary vein cross-section

From the previous position (Asc Ao short axis) retract the probe between 0° and 60° and rotate it clockwise. The right upper pulmonary vein (RUPV) and the right lower pulmonary vein (RLPV) are visualized. The RUPV is shown with a flow parallel to the US beam and can be evaluated on Doppler mode. Occasionally, a right middle lobar pulmonary vein can be viewed entering the LA between the RUPV and RLPV orifices. The evaluation of pulmonary veins is of special interest in congenital diseases.

Mid-esophageal aortic valve short axis cross-section

From the previously described view (right pulmonary vein) return to the Ao in the screen center with a counterclockwise rotation of the probe. Advance to AV commissural leaflets at an approximate angle of 45°. The general morphology of AV (number of valves, presence of calcifications, motion) is observed, besides determining if there is presence of aortic stenosis by planimetry. Interatrial septum (IAS) bulging continuously in the cardiac cycle by high pressures can also be observed in this window (Fig. 5A). From this position, the discreet withdrawal of the probe or its anteflexion also depicts the LAA.

Mid-esophageal right ventricle inflow-outflow cross-section

From the AV short axis, advance the probe and rotate the transducer angle between 50° and 70° until visualizing the TV, RV inflow tract (RVIT), RV outflow tract (RVOT), and proximal pulmonary artery. In addition, RA, LA, IAS, RV, and pulmonary valve (PV) are all observed. It is superior

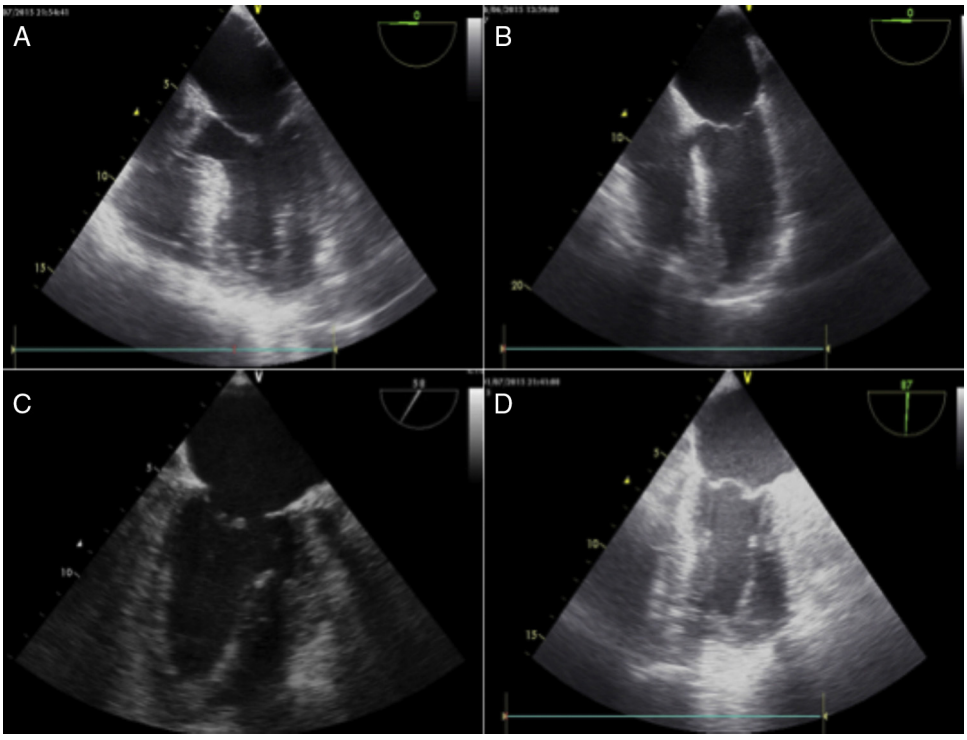

Figure 3 (A) Mid-esophageal five-chamber cross-section. (B) Mid-esophageal four-chamber cross-section. (C) Mid-esophageal commissural cross-section. (D) Mid-esophageal two-chamber cross-section.

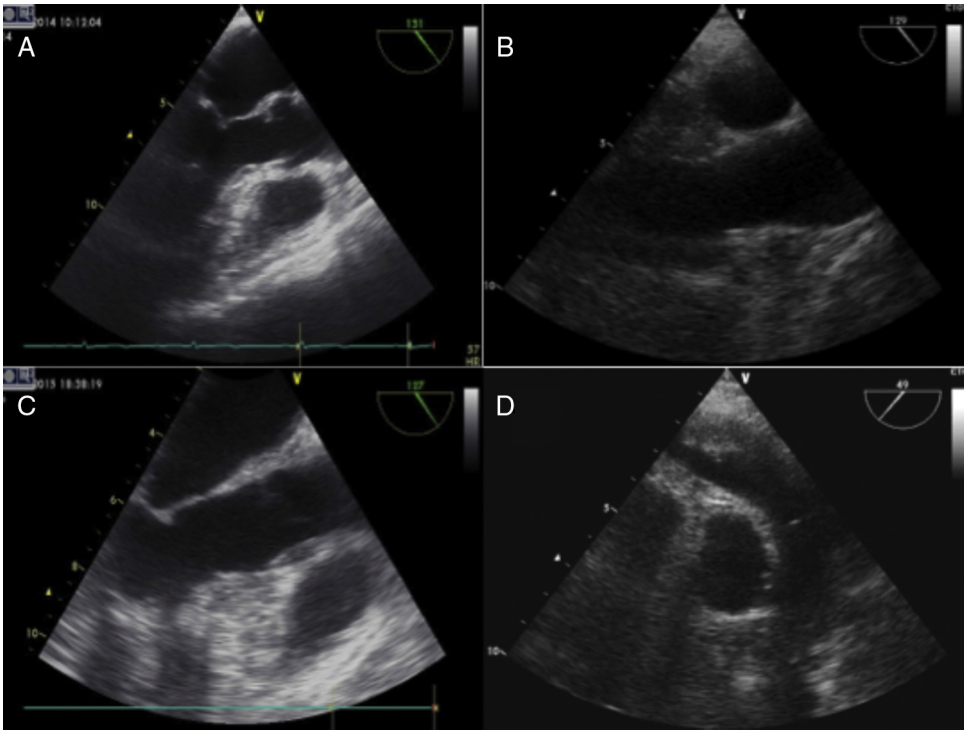

Figure 4 (A) Mid-esophageal long axis cross-section. (B) Mid-esophageal ascending aorta long axis cross-section. (C) Mid-esophageal aortic valve long axis cross-section. (D) Mid-esophageal ascending aorta short axis.

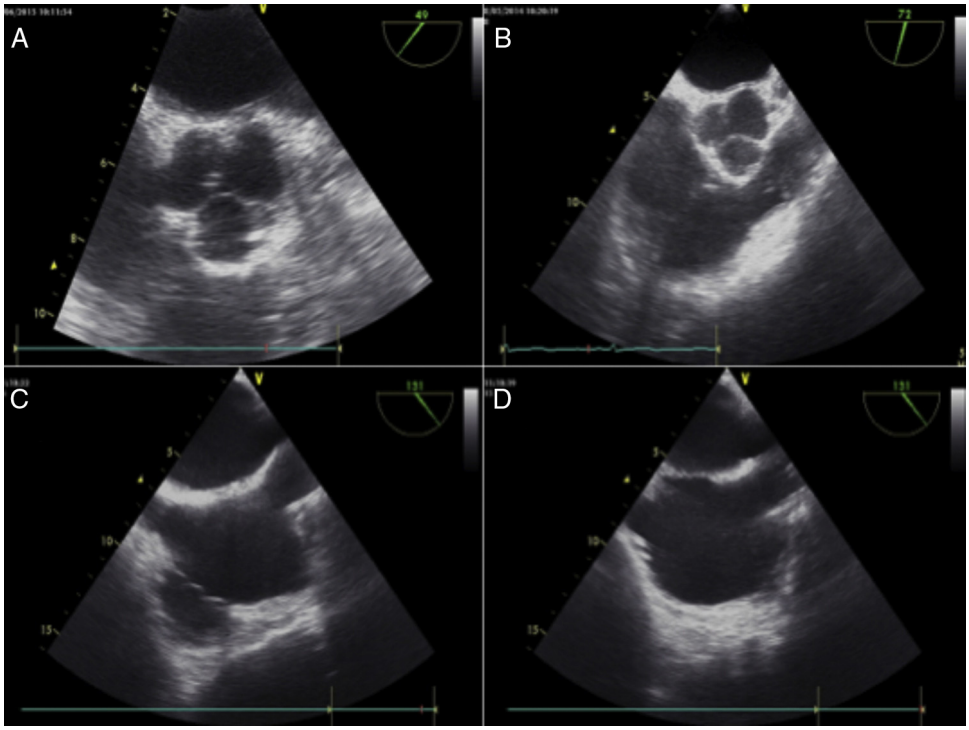

Figure 5 (A) Mid-esophageal aortic valve short axis cross-section. (B) Mid-esophageal right ventricle inflow-outflow cross-section. (C) Mid-esophageal modified bicaval cross-section. (D) Mid-esophageal bicaval cross-section.

when compared to the visualization of four chambers in the mid-esophagus plane for flow analysis by TV on Doppler mode. This window is also useful in congenital heart diseases and in the correct placement of pulmonary artery catheter (Fig. 5B).

Mid-esophageal modified bicaval cross-section

From the RVIT and RVOT window, with a clockwise rotation between 50° and 70°, TV is centralized and LA, IAS, RA and inferior vena cava (IVC) are visualized. It may be an apical window to analyze eccentric regurgitant jets by TV on Doppler mode (Fig. 5C).

Mid-esophageal bicaval cross-section

From the window previously described (modified bicaval) raise the angular rotation to 90–110° and rotate the probe clockwise. Structures to be analyzed include LA, IAS, RA, SVC, IVC, and right atrial appendage (RAA). This visibility position is especially important for analysis of PFO and IAS defects and to detect air within the atria, as well as to assist in the difficult passage of the pulmonary artery catheter into the RV (Fig. 5D).

Mid-esophageal right and left pulmonary veins cross-section

In the bicaval position in the mid-esophagus (90–110°) continue to rotate the probe clockwise until the right upper pulmonary vein (RUPV) and right lower pulmonary vein (RLPV) are visualized. When rotating the probe counterclockwise, the RUPV and RLPV can be visualized at the right end of the screen, where they are aligned parallel to the US sound beam. It is ideal for flow analysis on Doppler mode (Fig. 6A).

Mid-esophageal left atrial appendage cross-section

This cross-sectional view is obtained in the mid-esophagus with an angle between 90° and 110°, turning the probe clockwise. The upper left pulmonary vein (ULPV) is often visualized. Due to the complex and variable anatomy of the LAA, its evaluation must be done in different sections. Color Doppler and pulsatile Doppler are useful modalities of evaluation, particularly regarding the LAA contractile function (Fig. 6B).

Transgastric basal short axis cross-section

From mid-esophagus, the probe is advanced to the stomach and maintains the zero angulation. During the probe introduction, CS and TV are often visualized. Once in the stomach, this cross-section is obtained with a slight anteflexion of the probe. Its characteristic image is the MV on its short axis (fish mouth), with the anterior cusp on the left and the posterior cusp on the right. MV morphology and LV size and function can be assessed. In patients with mitral regurgitation, the use of color Doppler can be useful to characterize its regurgitant orifice (Fig. 6C).

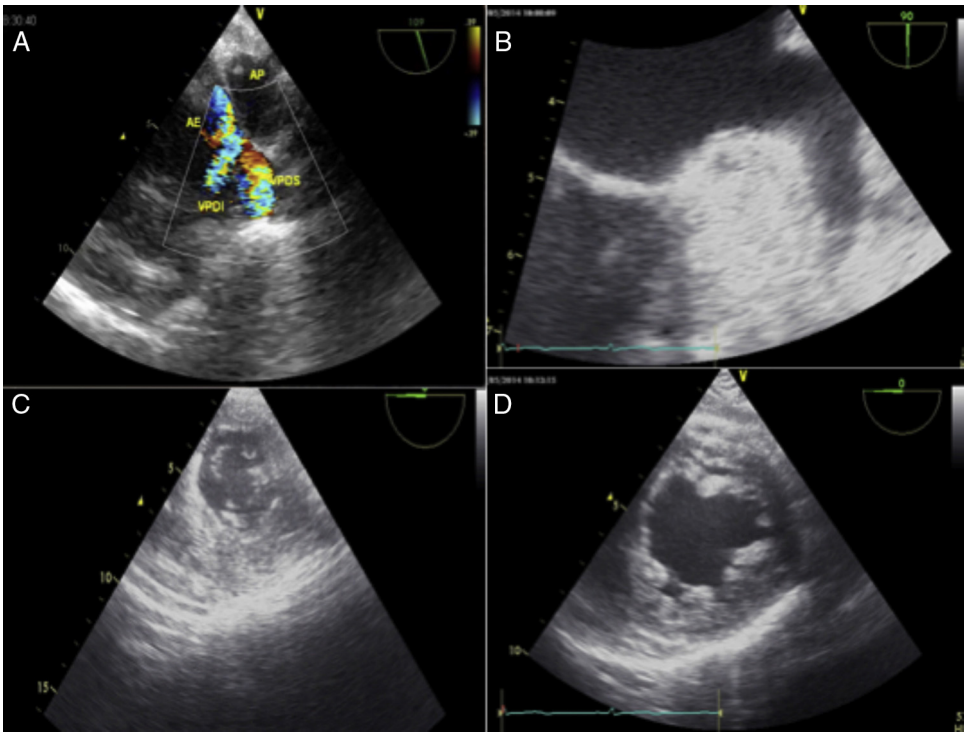

Figure 6 (A) Upper-esophageal right and left pulmonary veins cross-section. (B) Mid-esophageal left atrial appendage cross-section. (C) Transgastric basal short axis cross-section. (D) Transgastric mid-papillary short axis cross-section.

Transgastric mid-papillary short axis cross-section

From TG basal short axis cross-section, the probe should return to the neutral position, or be minimally advanced, maintaining the zero angulation. This cross-section is extremely useful in assessing and monitoring the volume and size of regional and global LV function, as well as assessing territories irrigated by the right coronary (RC), anterior descending (AD), and circumflex (Cx) arteries. In it, the anterior, inferior, inferolateral, anterolateral, and septal walls can be identified, as well as the papillary anterolateral and posteromedial muscles (Fig. 6D).

Transgastric apical short axis cross-section

Maintaining contact with the gastric wall, the probe is slightly advanced and/or retroflexed from the TG mid-papillary short axis, favoring the visualization of the apical segments of the LV and RV (turning the probe clockwise). This cross-section may be difficult to obtain due to the possible loss of contact between the probe and the gastric wall caused by retroflexion of the probe (Fig. 7A).

Transgastric right ventricular cross-section

This image is obtained at the same level as the TG basal short axis cross-section, only turning the probe clockwise. TV is visualized on its short axis. The use of color Doppler in this cross-section may help to characterize the TV regurgitant orifice (Fig. 7B).

Transgastric right ventricular inflow-outflow cross-section

This image is orthogonal to that described previously (simply rotate the transducer by 90°). The anterior and posterior TV cusps and left and right PV valves are usually visualized. This cross-section can be used to align the jets in PV with the US beam for use in the continuous and pulsatile Doppler modes (Fig. 7C).

Deep transgastric five-chamber cross-section

This image is obtained by advancing the probe in the stomach, maintaining contact with the gastric wall (probe anteflexion). It is the ideal incidence for Doppler analysis of AV, LVOT, and often MV, as blood flow is parallel to the US beam (Fig. 7D).

Transgastric two-chamber cross-section

This cross-section is obtained from TG mid-papillary short axis, changing the angle to 90°. It allows evaluation of the LV anterior and inferior walls, as well as the entire mitral valve apparatus (MV, papillary muscles, *chordae tendineae*). It is also possible to visualize the LA and the LAA (Fig. 8A).

Transgastric long axis cross-section

This cross-section is obtained by advancing the angle to 120–150° from TG two-chamber. Portions of the inferolateral and anterior septal walls, LVOT, AV, and proximal Ao

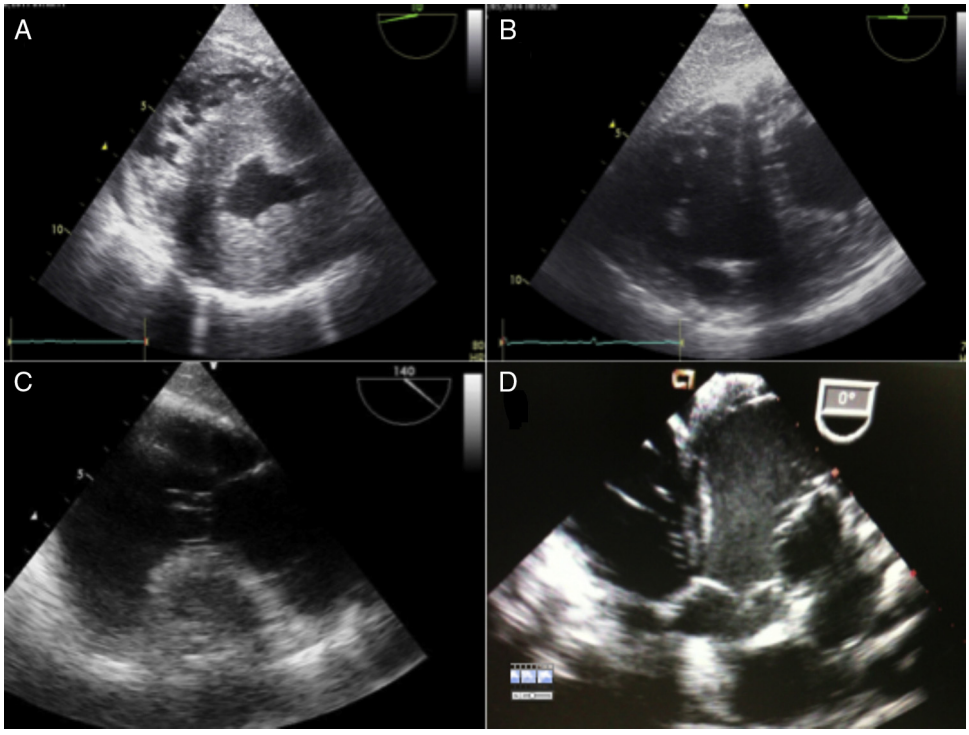

Figure 7 (A) Transgastric apical short axis cross-section. (B) Transgastric basal right ventricle cross-section. (C) Transgastric right ventricle inflow-outflow cross-section. (D) Deep transgastric cross-section.

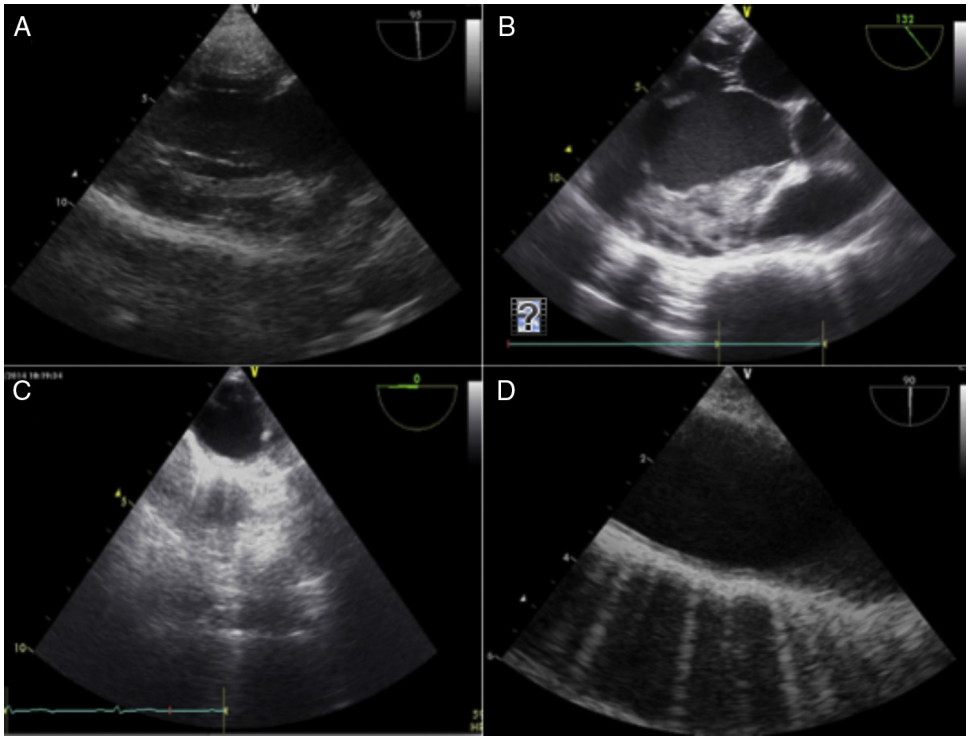

Figure 8 (A) Transgastric long axis cross-section. (B) Transgastric long axis cross-section. (C) Descending aorta short axis cross-section. (D) Descending aorta long axis cross-section.

are visualized. Because LVOT and AV are parallel to the US beam, a Doppler analysis is possible (Fig. 8B).

Descending aorta long and short axes cross-section

Because the descending aorta (Desc Ao) is adjacent to the esophagus and stomach, the acquisition of images is simple. From TG mid-papillary short axis cross-section, the probe should be rotated at about 180°, with slight adjustments until the abdominal Ao (below the diaphragm) is visualized, at the celiac trunk level; the probe is drawn and the transducer angle is maintained at zero degree and the short axis is obtained; the long axis is obtained with the transducer angle at 90°. Image quality can be improved by decreasing the depth and adjusting the gain. Because there are no internal anatomical structures in Desc Ao, the description of findings location is usually based on the distance from the finding to the incisor teeth. Another important factor in the Desc Ao evaluation is the hemiazygos vein presence, which drains the posterior left thorax, often visualized in the most distal field of the image, joining the upper thorax to the azygos vein, which drains the right thorax. The azygos vein, being normally parallel to Ao and its walls being contiguous, can often be erroneously identified as a dissecting aortic blade. Color and pulsatile Doppler analysis easily differentiates the arterial from the venous flow (Fig. 8C and D).

Upper esophageal aortic arch long axis cross-section

This image is obtained from the Desc Ao short thoracic axis; the probe is withdrawn until Ao becomes elongated and the left subclavian artery emergence is visualized. This position indicates the end of the distal aortic arch. The probe is turned clockwise and it is possible to visualize the mean aortic arch and the left innominate vein. Because the left source bronchus interposes between the esophagus and Ao, it is usually not possible to visualize the proximal aortic arch and the distal Asc Ao (Fig. 9A).

Upper esophageal aortic arch short axis cross-section

From the cross-section described above, the transducer angle is increased to about 70–90° to obtain the long axis. The pulmonary artery trunk and PV can be visualized on the long axis; it is possible to obtain Doppler measurements. Due to Ao curvature, the right brachiocephalic trunk and left common carotid artery can often be identified to the right on the monitor (Fig. 9B).

Mitral valve

Introduction

Among the cardiac valves, MV has the most favorable anatomic characteristics for transesophageal examination, as the near field is close to the transducer, has the LA as an ''acoustic window'', and has no cardiac structure that can be calcified and/or generation of acoustic shadow between the transducer and its structure[11] (Fig. 1).

During the MV intraoperative period, TEE is a fundamental tool, as it allows the lesion identification and a detailed description of its mechanism and severity, thus helping the surgical decision making.[11]

Anatomy and nomenclature

When studying the MV anatomy and function, the most correct is that it is viewed as a valve complex composed of distinct anatomical structures that work in a coordinated way for its correct functioning.[12] The mitral valve complex, or mitral valve apparatus, is composed of mitral annulus, cusps, *chordae tendineae*, papillary muscles, and the left ventricular musculature.[12]

Mitral annulus

The mitral annulus is a connective tissue structure with a three-dimensional saddle-shaped complex structure. It is anteriorly related to the aortic valve apparatus, joins the atrium and left ventricle, and receives along its perimeter the insertion of the valvular cusps.[12]

Mitral annulus has two main axes, one anteroposterior (upper and shorter) and one commissural (lower and longer). These axes may also be referred to as anteroposterior and anterolateral–posteromedial[13] (Fig. 10A and B).

Under the ventricular contraction action, the mitral annulus posterior region undergoes a significant reduction of its total area, with reduction up to 25%. The mitral annulus anterior region folds during systole and further decreases the anteroposterior diameter.[13]

Leaflets (cusps)

The normal mitral valve complex is composed of two anterior and posterior leaflets.[12,13] The anterior leaflet is inserted into the anterior annulus, in a fibrous skeleton region adjacent to the aortic valve apparatus, called mitral-aortic intervalvular fibrosa (MAIVF). It occupies approximately 1/3 of the annular perimeter and 2/3 of its area. The posterior leaflet inserts into the posterior annulus and occupies 2/3 of its perimeter, but corresponds to only 1/3 of the annular area.[13,14] The leaflets are in a curved coaptation line along the intercommissural axis (anterolateral–posteromedial); in normal situations, there are approximately 1 cm of tissue overlap.[12]

MV leaflets were subdivided into distinct regions in order to improve communication among medical team members. Among the proposed schemes, we will use Carpentier nomenclature,[10] which is also used by ASE and SCA.[1]

According to Carpentier nomenclature, MV is subdivided into eight regions, from anterior to posterior, through small grooves or indentations present in the posterior leaflet. The posterior leaflet is divided into three segments, which are numbered from 1 to 3, with P1 being the most anterior and P3 the most posterior.[10] The anterior leaflet usually has no real anatomical grooves; however, didactically, it is subdivided in the same way as the posterior one: a more

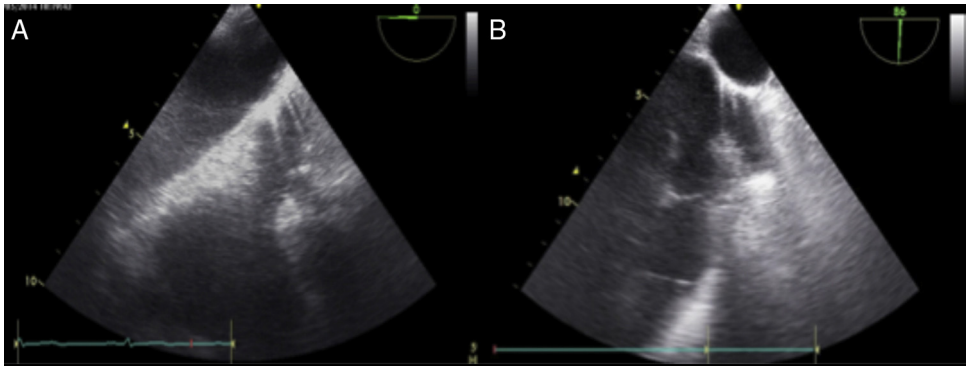

Figure 9 (A) Upper-esophageal aortic arch long axis cross-section. (B) Upper-esophageal aortic arch short axis cross-section.

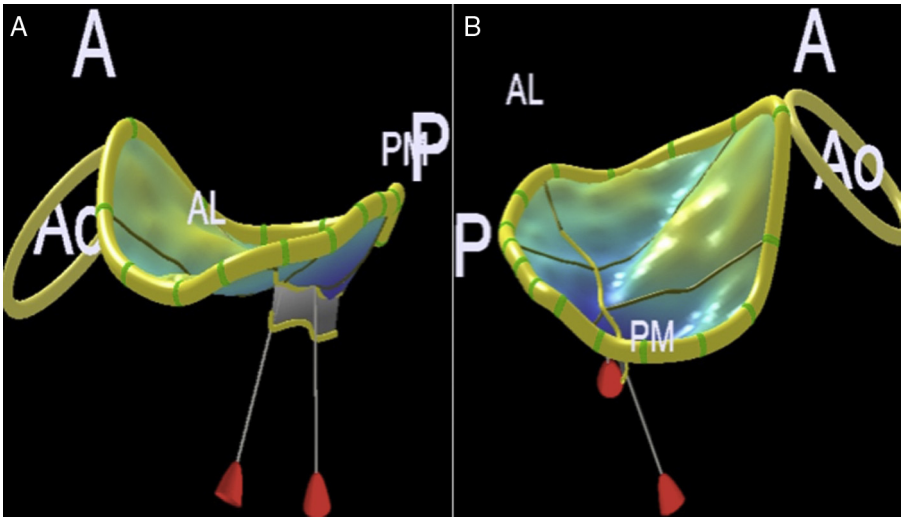

Figure 10 Mitral annulus assessment by three-dimensional echocardiography. (A) Anteroposterior diameter. (B) Anterolateral–posteromedial diameter. Ao, aortic ring; A, anterior; P, posterior; AL, anterolateral; PM, posteromedial.

anterior region (A1), a middle region (A2), and a posterior region (A3). At the anterolateral and posteromedial ends, two regions are defined as anterolateral commissure and posteromedial commissure, respectively[10] (Fig. 11).

Papillary muscles, *chordae tendineae*, and left ventricle

The two papillary muscles (anterolateral and posteromedial) support the leaflets, located parallel to the ventricular musculature.[12] The anterolateral muscle generally arises from the middle portion of the anterolateral LV wall, receives vascularization from the AD and Cx artery branches. The posteromedial papillary muscle arises from the middle portion of the inferior wall, is exclusively vascularized by the RC artery branch, which makes it more vulnerable to ischemic insult.[12]

The *chordae tendineae* connect both the papillary muscles and ventricular musculature to the MV leaflets. The anterolateral papillary muscle supports, through its cords, the A1/P1 segments and the anterolateral portion of the A2/P2 segments; the A2/P2 posteromedial portion and the A3/P3 segments are supported by the posteromedial papillary[12] (Fig. 12).

Chordae tendineae are classically divided into first, second and third-order chordae. First-order *chordae* are connected to the tip of the leaflets, having as a consequence of its rupture the systolic eversion of leaflets, echocardiographically known as flail.[12,13] Second-order *chordae* are connected to the base of leaflets and are known as structural *chordae*; it is possible to identify two to four chordae thicker than the others.[12,13] Third-order *chordae* usually connect the posterior MV leaflet to the left ventricle wall, having recognized importance in architecture maintenance and ventricular performance[12] (Fig. 12).

Intraoperative mitral valve echocardiographic examination

In order to include and standardize the intraoperative use of new technologies that emerged in the last decade, mainly real-time three-dimensional (3D) TEE, in addition to the inclusion of new imaging plans, the 1999 ASE/SCA guidelines were reviewed and republished in 2013.[1,2,15] Such patterns

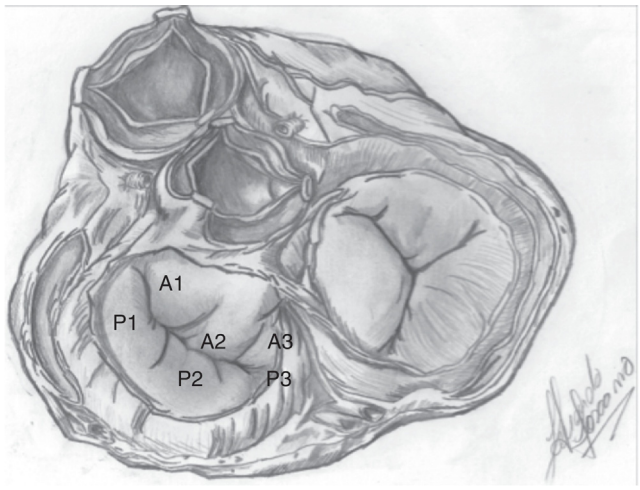

Figure 11 Carpentier nomenclature: segments #1 are anterolateral, #3 are posteromedial, and #2 correspond to the valve mid-portion. The anterior and posterior commissures are also visualized.[12]

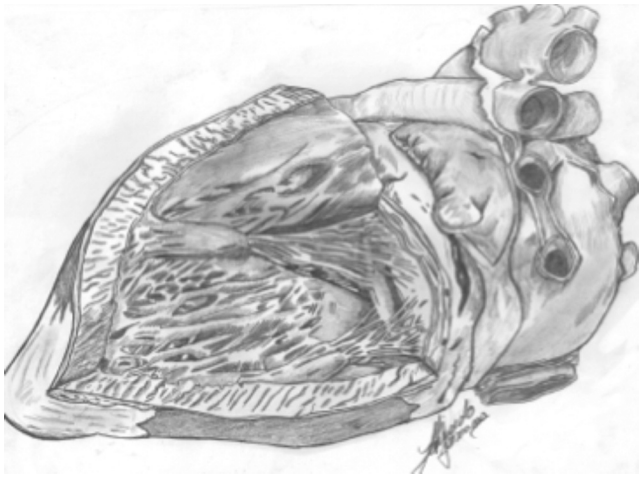

Figure 12 Mitral subvalvar apparatus, showing the *chordae tendineae* distribution at each cusp.[12]

of image acquisition and training were also adopted by the SBA for teaching and training.[4]

Didactically, we will describe the MV sequential evaluation method through the ASE/ACS methodology,[1] trying to identify its different segments according to their clinical importance. It is known that its accuracy is variable and highly dependent on the examiner's experience, as demonstrated by Mahmood et al.[16] On the other hand, the ability to localize it spatially in the mitral apparatus anatomy using two-dimensional (2D) examination still requires fundamental training.

Mid-esophageal five-chamber cross-section
With the probe insertion at a depth of approximately 30 cm, with multiplane angle rotation about 10°, AV, LVOT, LV (except its apex), and A1–A2 and P1–P2 segments are visualized (Fig. 3A).

Mid-esophageal four-chamber cross-section
The probe is inserted at a depth of approximately 35 cm, with multiplane angle rotation between 10° and 20°, until MV can be clearly visualized. The segments A3–A2 and P2–P1 are evident, as well as the TV septal and posterior leaflets (Fig. 3B).

Mid-esophageal commissural cross-section
With the probe in the four-chamber position, the multiplanar angle is advanced between 50° and 70° and the commissural plane will be visualized. The segments P1, A2, and P3 will be visible from right to left, in addition to the papillary anterolateral and posteromedial muscles. The probe is rotated to the right and the image plane will pass through the entire extension of the anterior leaflet (right commissural: A1–A2–A3), as well as the entire extension of the posterior leaflet when rotated to the left (left commissural: P1–P2–P3, Fig. 3C).

Mid-esophageal two-chamber cross-section
From the commissural plane, the multiplane angle is advanced between 80° and 100° and the image plane called two-chamber will appear. From right to left, the MV segments will be A1/A2/A3 and P3 (Figs. 3D and 4A).

Transgastric basal short axis cross-section

The transducer is advanced to the stomach, with the multiplane angle between zero and 20°, and a MV image is obtained with a fish mouth opening and closing. The anterior leaflet appears to the left and the posterior leaflet to the right; the posteromedial commissure appears near the transducer and the anterolateral commissure more distal to the transducer (Fig. 6C).

Three-dimensional frontal cross-section (face view)
MV apparatus 3D evaluation is useful for defining and locating the pathology, describing the pathophysiological mechanism and its severity, as well as facilitating communication with the interventional surgeon or cardiologist.[1] With the evolution of surgical and percutaneous techniques of mitral apparatus repair there was a need for real-time high quality images, which is now possible thanks to the technological evolution of the matrix array and image manipulation softwares.[17]

The complete 3D examination will be treated in a specific topic, but we will describe two more representative and useful intraoperative imaging plans, which may be in real-time or in multi-beat acquisitions.

Left atrium view or surgeon's view
From the LA view, it is possible to identify all the valve segmentation, which facilitates the topographic description of a pathology and communication with the surgical team. By convention, AV is positioned at 12 o'clock in the image and LAA at 9 o'clock (Fig. 13A and B).

Left ventricle view
In the left ventricular aspect, the imaging plane should again be oriented with LVOT and AV positioned at 12 o'clock, with posterior leaflet at the bottom of the image, anterior leaflet

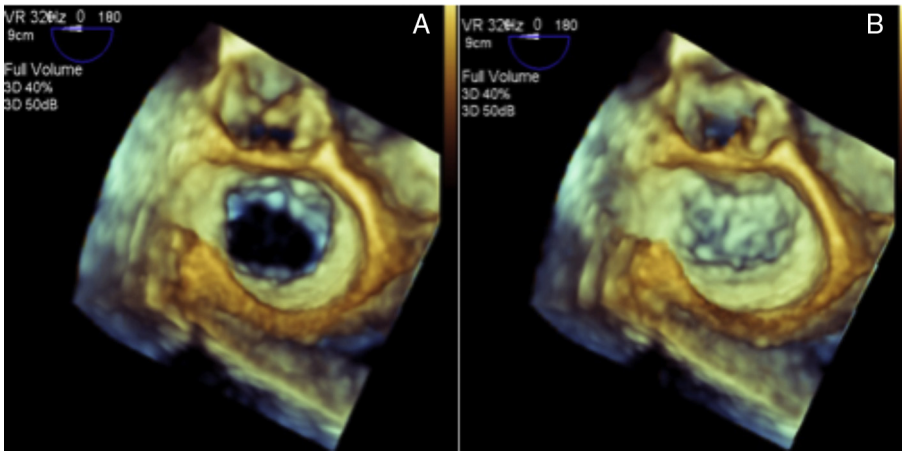

Figure 13 Mitral valve view in three-dimensional image. (A) Mitral valve in diastole. (B) Mitral valve in systole.

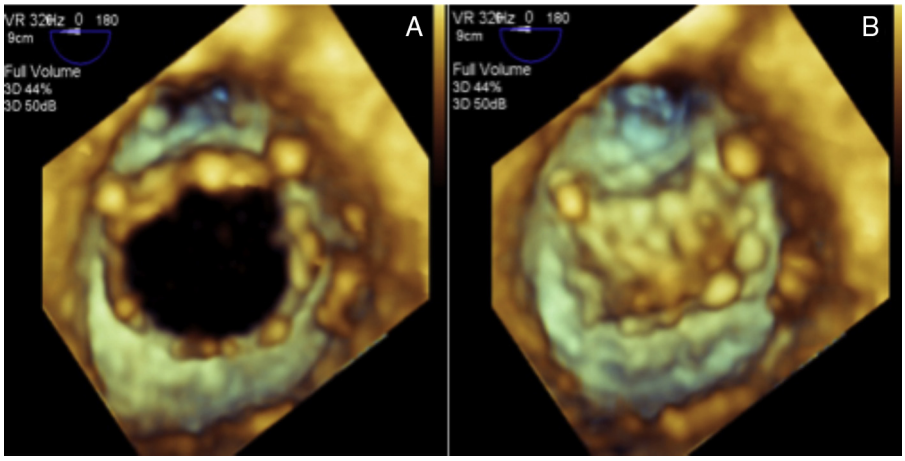

Figure 14 Mitral valve view of left ventricle in three-dimensional image. (A) Mitral valve in diastole. (B) Mitral valve in systole.

at the top, anterolateral commissure to the right, and posteromedial commissure to the left (Fig. 14A and B).

3D color Doppler echocardiography

By means of multi-beat acquisition, it is possible to obtain volumetric images of the regurgitant jet and its relation with the MV structures and 3D evaluation of its various components, which allows to demarcate its exact location and quantitative evaluation in specific software[18] (Fig. 15).

Three-dimensional quantitative evaluation of mitral valve

Besides the ability to generate real time 3D images, numerous software were developed with the ability to generate a quantitative analysis model from specific points marked on the 3D image of the valve apparatus. Among these, the most widely used and studied software are Mitral Valve Quantification – MVQ (Phillips Healthcare®, Inc., Andover, MA) and 4D MV–Assessment Software (TomTec Imaging Systems GmbH®, Munich, Germany).[18] Although reference values and clinical usefulness are still in the validation stage, important knowledge has been accumulated regarding mitral valve apparatus remodeling in different pathophysiological states.[18]

Intraoperative evaluation of mitral valve

The evaluation objectives before cardiopulmonary bypass are to define the mechanism, locate the lesion, estimate its severity, and identify associated pathologies, such as pulmonary arterial hypertension, ventricular dysfunction, and tricuspid regurgitation.[13] It should be noted, however, that general anesthesia significantly modifies the hemodynamic conditions and often decreases the severity of regurgitant valve lesions.[13]

Evaluation of annular morphology

Different clinical situations and pathologies alter the annular dimensions. By definition, mitral annulus should be measured in the mid-esophagus, long axis at the end of systole. The measurement is made from the insertion of posterior leaflet to the AV base. The upper limit of normality is 35 mm, values greater than 40 mm indicate marked dilatation.[13] The intercommissural diameter is often also measured, but its reference values are less clear in the literature[13] (Fig. 10A and B).

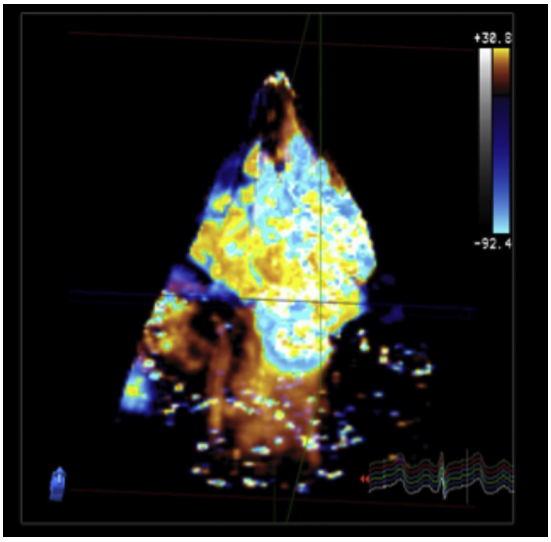

Figure 15 Three-dimensional color Doppler of mitral valve.

Leaflets evaluation

MV diseases can be classified according to the leaflets motion, according to Carpentier's classification.[10,19]

Diseases are classified as type I if presenting with normal leaflet motion, such as mitral regurgitation due to endocarditis leading to leaflet perforation, congenital clefts or isolated annular dilatation, in case of atrial fibrillation[19]; type II if presenting with excessive leaflet motion, such as prolapse caused by fibroelastic deficiency or Barlow's disease[19]; and type III when presenting with a pathophysiological mechanism that causes restricted leaflet motion and may be subdivided into IIIa, IIIb, and IIIc. The IIIa subtype corresponds to restriction caused by shortening and fusion of the subvalvar apparatus, such as in rheumatic heart disease. The IIIb and IIIc subtypes represent restriction due to leaflet tethering, as in functional mitral regurgitation, with IIIb corresponding to symmetric and IIIc to asymmetric tethering[19] (Fig. 16B and C).

Mitral regurgitation caused by type II pathologies in general produce regurgitant jets in the opposite direction of the lesion; however, central jets may occur in case of both leaflets involvement.[19]

Type III pathologies, with restricted leaflet motion, usually produce regurgitant jets in the same direction as the leaflets, may be central in case of symmetrical involvement.[19]

Systolic anterior motion

Systolic anterior motion (SAM) of MV has been reported after valve repair, with an incidence up to 16% in patients with myxomatous disease.[20] It consists of the anterior displacement of the coaptation point and subvalvular tissue toward LVOT during systole, causes varying degrees of dynamic obstruction[20] (Fig. 17).

Not all SAM causes clinically relevant obstruction. It is traditionally diagnosed in the presence of a gradient across the LVOT and mitral insufficiency.[20] The presence of mitral tissue across the LVOT is often possible to be verified, but without any gradient, a situation clarified by 3D/4D TEE.[14] The ability to echocardiographically predict which patients are at greatest risk for SAM development after mitral repair is a key task of intraoperative examination. In the last two decades, some criteria have been defined and validated. The most relevant ones are the following:[20–22]

- Distance between coaptation point and septum (5-chamber long axis) <2.5 cm;
- Posterior leaflet systolic length (5-chamber long axis) >1.5 cm;
- Relationship between anterior/posterior systolic length (5-chamber long axis) <1.4 cm;
- Small ventricular cavity – diastolic diameter <4.5 cm;
- Interventricular septum (IVS) bulging >1.5 cm;
- Mitroaortic angle (3D quantification) >65° at rest and >35° under stress;
- Aortomitral angle (3D quantification) <120°.

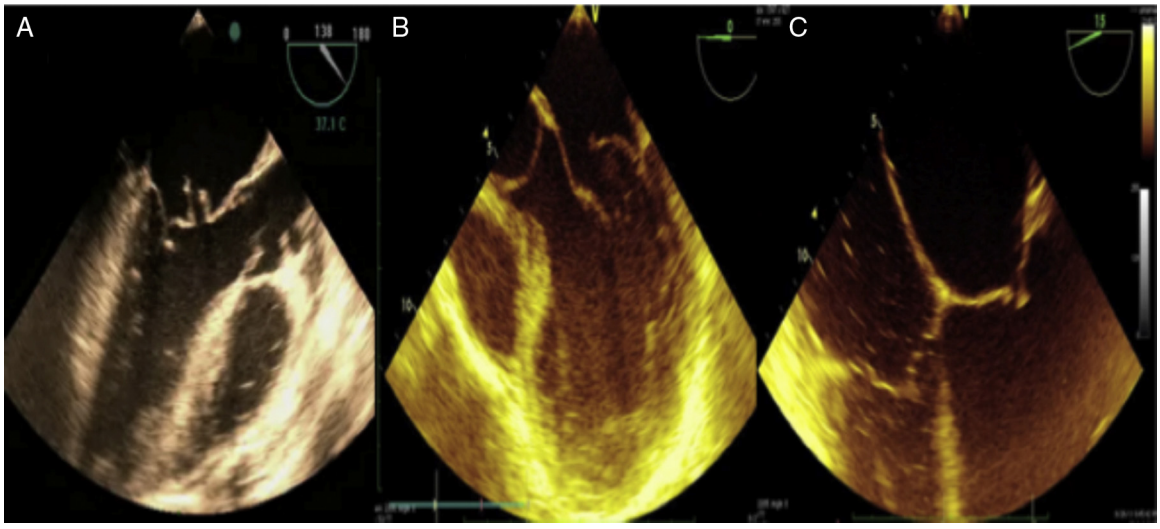

Figure 16 Carpentier classification: (A) normal motion; (B) excessive motion; (C) restricted motion.

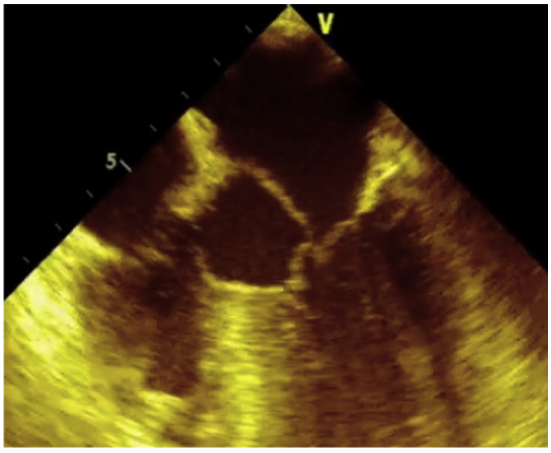

Figure 17 Mitral valve anterior systolic motion.

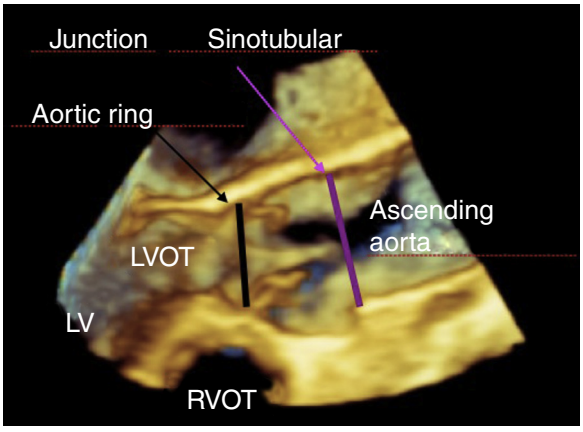

Figure 18 Aortic complex. LV, left ventricle; LVOT, left ventricular outflow tract; RVOT, right ventricular outflow tract.

Left ventricular outflow tract, aortic valve and aorta

AV is a component of the aortic root, which by definition extends from the basal aortic valve annulus to the sinotubular junction. With the association of the LVOT interval triangles, we will have the so-called aortic valve complex[23] (Fig. 18). Pathologies can occur not only in AV but also involve any components of this complex, which reinforces the importance of a detailed, hemodynamic, and anatomical evaluation of this region.[1] With the advent of new technologies for treating aortic complex pathologies, there was a great advance in the understanding of its anatomy; 2D and 3DD TEE stand out in the detailed morphological evaluation of these anatomical structures.[24]

Anatomy

The aortic valvar complex is a continuation of the LVOT and is located to the right and posterior to the RVOT, with its posterior margin wedged between MV orifice and muscular IVS.[24] Its basal circumference is called aortic annulus or basal ring (Fig. 18) and has an oval shape in most individuals.[24–26]

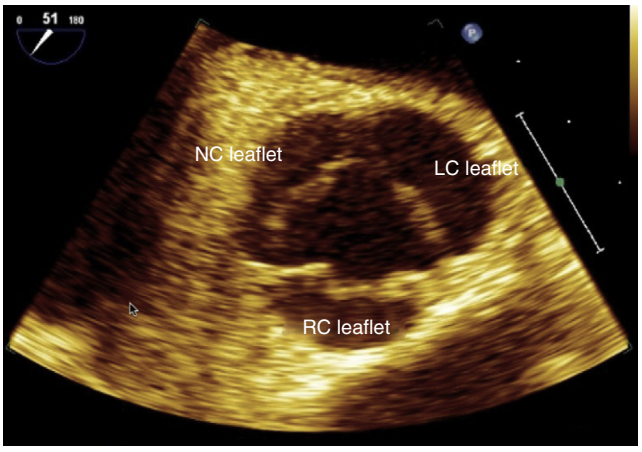

Figure 19 Mid-esophageal aortic valve short axis cross-section. NC, non-coronary; LC, left coronary; RC, right coronary.

Approximately two thirds of this basal ring, where the AV valves nadirs are inserted, are connected to the muscular IVS and the remaining third is in contact with the mitral valve anterior leaflet, represents the base of a fibrous triangle between the non-coronary valves and left coronary artery (''fima'').

The aortic root extends from the aortic valves basal insertion to the sinotubular junction, passes through the Valsalva sinuses, from where on the upper border of the left and right coronary sinuses the coronary arteries originate. Thus, AV is a semilunar valve with three valves, identified according to the presence or absence of a coronary artery, which originates from the corresponding sinus of Valsalva: left coronary valve, right coronary valve, and non-coronary valve[24] (Fig. 19).

2D and Doppler imaging of aortic valve and left ventricular outflow tract

Its anatomical location close to the LA, which is in contact with the esophagus in its mid-plane, provides a precise anatomical image, both in short (Fig. 5A) and long axes views (Fig. 4B).[24] The perpendicular contact of the US beams with these near field allows us to use the highest available frequencies, with consequent detailed appreciation of their morphology.[5] The use of zoom as a resource to increase the detail for distance and/or diameters measurements can further improve accuracy and is recommended (Fig. 20). The Doppler bundles perpendicularity with these structures in the mid-esophagus echocardiographic sections makes it impossible to accurately assess the flow velocities.[5] This limitation is overcome with TG long axis (Fig. 8B) and deep TG sections (Fig. 7D), in which the parallel alignment with the beams allows an accurate assessement.[5,27]

Mid-esophageal aortic valve short axis cross-section

Obtained with a slight 25–45° angulation, the three AV valves can be evaluate, with the right coronary valve in

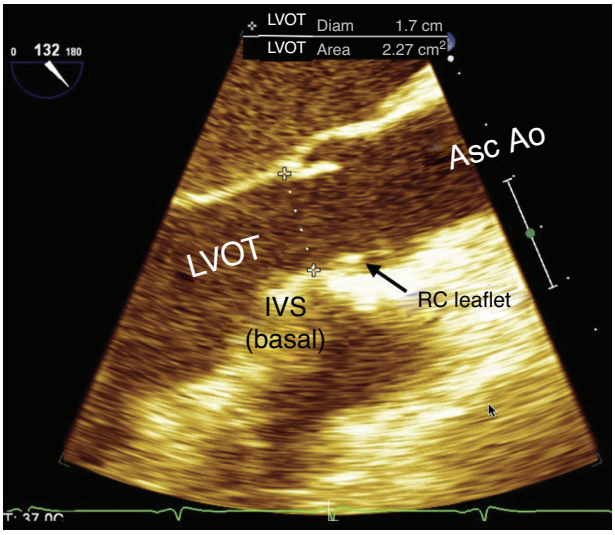

Figure 20 Mid-esophageal aortic valve long axis cross-section. LVOT, left ventricular outflow tract; IVS, interventricular septum; RC, right coronary; Asc Ao, ascending aorta.

the most anterior position, non-coronary valve adjacent to the IAS, and left coronary cusp positioned laterally to the left (Fig. 19). This cross-section presents excellent spatial and temporal resolution, allowing a detailed view of the valve shape and function, which is important to evaluate the valvar dysfunction mechanisms. Color Doppler flowmetry is applied to assess aortic regurgitation and the size, mechanism, and position of the regurgitant orifice.[28] Probe removal or anteflexion can display the left coronary ostium image, as well as its introduction or retroflexion can provide an image of the LVOT short axis.

Mid-esophageal long axis cross-section

The multiplane angle is rotated to 120°, from the mid-esophagial four-chamber cross-section, and the basal portion of IVS, LVOT, aortic root (aortic ring, Valsalva sinus, and sinotubular junction), and Asc Ao proximal tubular portion appears on the right side of the image (Fig. 20). Two AV valves are displayed, the right coronary is always that most distal to the transducer because it is the most anterior. The other cusp present in this cross-section may be the left coronary, or most often the non-coronary, depending on the commissure position between them and the exact location of the imaging plate as it passes through the AV. Presence of calcification, thickening, motion degree, and valve opening, as well as its anatomical relationship with adjacent structures, such as coronary ostia and IVS, should be evaluated. The basal aortic ring diameter measurement is made in this cross-section using 2D TEE, preferably with zoom image, as the distance between the most ventricular nadir of the right coronary valve and the base of the fibrous triangle (''fima''), contralateral and orthogonal to the aortic root longitudinal axis, in the ventricular systole. This measure is usually smaller than that of the coronal axis (only obtained via 3D TEE or tomography) due to the basal ring oval shape. This evaluation accuracy is important for hemodynamic measures of systolic volume and cardiac output, as well as for predicting the size of aortic, percutaneous, or surgical prostheses placed in this region.[27] In addition, the diameters of the other components of the aortic root, as well as that of Asc Ao, should be measured. In case of aortic stenosis, where there is proximal flow convergence, the LVOT diameter (located approximately 5 mm before the aortic ring) should be used – pulsed-Doppler sample volume is placed in the same site to calculate the systolic volume ejection.[29] In this cross-section, the perpendicularity of the US beam incidence in this region flow does not allow accurate velocity measurements with pulsatile and/or continuous Doppler.[28] In contrast, color Doppler measurements are useful and reliable, providing important information, such as: turbulent flow regions with LVOT obstructions; measurement of vena contracta regurgitant jet; and relation between regurgitant jet diameter and LVOT diameter.[28]

Transgastric long axis and deep transgastric cross-sections

These cross-sections are essential in the assessment, allowing accurate alignment of LVOT and AV flows, with reliable measurement of their velocities through continuous and pulsed Doppler modes, important for gradation of valvar and/or subvalvular stenoses, regurgitant jets, and measurement of LV ejected systolic volume (Figs. 7D and 8B).[27,28]

In this cross-section, evaluations of anatomical structures lose spatial resolution because they are distant from the focus and parallel to the US bundle, the complementary action of trangastric cross-sections with mid-oresophageal cross-sections is emphasized in the complete assessment of AV and LVOT and measurement of ejection systolic volume and cardiac output.

2D imaging and Doppler of ascending aorta

The necessary cross-sections for Asc Ao complete evaluation are the following: mid-esophageal ascending aorta long axes and short-axes. As mentioned previously, due to the perpendicular incidence of US bundle, these cross-sections have optimal spatial resolution and serve for measurement of Valsalva sinuses, sinotubular junction, and ascending aorta proximal tubular portion.[27] Simultaneous orthogonal cross-sectios using 3D transducers are useful for certainty of correct spatial orientation. When measuring Ao diameter, it is particularly important to measure the largest diameter perpendicular to the vessel long axis in that cross-section.[30] Measurements should be made using 2D image because of the risk of underestimation when using M mode, due to the systolic movement of the base of the heart in the apical direction (mean variation of 2 mm in the sinus of Valsalva diameter).[31,32] Color Doppler of these regions is important in the identification of abnormal flow turbulences and characterization of pathologies, such as aortic dissection, intramural hematomas, and other acute aortic syndromes.[28]

2D imaging and Doppler of descending aorta

From TG plane to upper esophageal plane, Ao can be visualize by rotating the probe in the posterior direction and adjusting the image to a depth of 6 cm. From TG plane, the probe is withdrawn in small increments while the proximal abdominal Ao and its branches, such as the renal artery, are evaluated[33] (Fig. 21), as well as the thoracic descending Ao along its length, stopping for a better analysis if there is any clinically significant lesion (Fig. 22). From gastric plane to mid-esophagial plane, the transverse image of Ao is generated at zero degree. When reaching the upper esophagus, the aortic arch appears in longitudinal view, due to its anatomical position at that level (Fig. 9A). If in this plane the angle is turned to approximately 90°, the left subclavian artery exit can be evaluate and, turning the probe to the left, part of its extension can be evaluated (Fig. 9B). With an anti-clockwise rotation, the two other brachiocephalic vessels can be evaluate. The innominate artery view is the most difficult because it is located in a blind spot where the trachea interposes.[34] The use of *X*-plane, available in 3D transducers, allows the thoracic Ao evaluation in both longitudinal and transverse planes simultaneously, improves the time needed for evaluation, and generates an image with correct spatial orientation of plaques that may be present and need to be evaluated.[35] Color Doppler image of thoracic Ao is used for abnormal flow evaluation, particularly in acute aortic syndromes. Pulmonary Doppler is used to identify holodiastolic reflux, an important component of qualitative gradding of aortic regurgitation (Fig. 23).[28] Due to the variable anatomical relationship between the esophagus and thoracic Ao, it is difficult to determine the anterior-posterior and right-left orientations on echocardiographic images of this region. The definition of its relation with adjacent anatomical structures, such as LA, pulmonary vein, pulmonary artery, and LV becomes a useful tool for this position definition.[1]

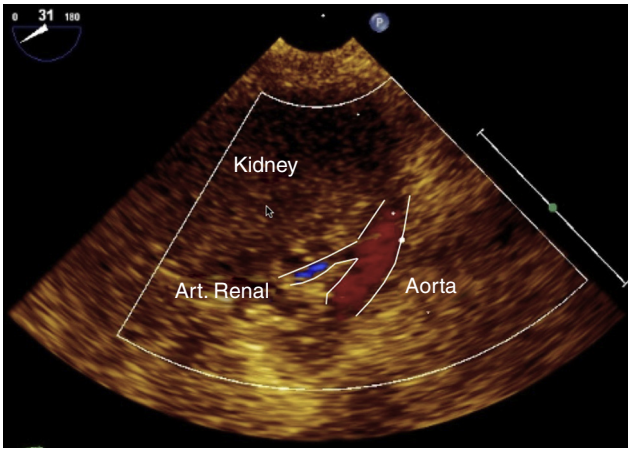

Figure 21 Renal artery cross-section.

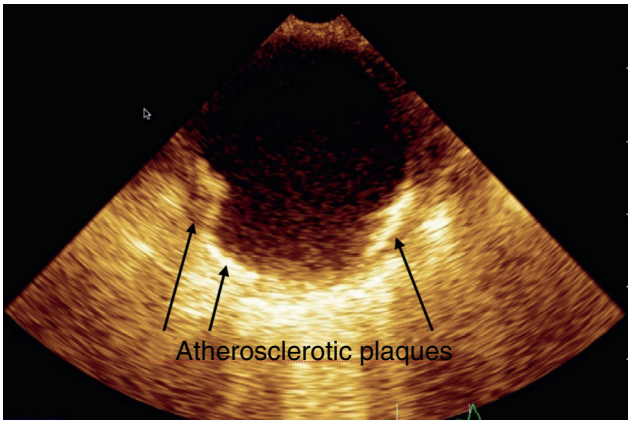

Figure 22 Atheroma plaques in descending aorta short axis.

3D imaging of aortic valve and aorta

The 3D echocardiographic image is acquired by capturing an anatomical image volume (Fig. 24), defined in its size by the operator, unlike the 2D echocardiography acquired by slices of these images.[36] This volume contains a more accurate information on the region of interest, allows the collection of detailed information through an ''electronic dissection'' of the aquired volume.[36] This captured volume allows the acquisition of two-dimensional image slices, with spatial orientation appropriate to the desired information, through a resource called multiplane reconstruction[37,38] (Fig. 25). However, by acquiring more ultrasound information at each capture, we have a loss in temporal resolution proportional to the size of our region of interest. With this kept in mind, we must always balance the temporal and spatial resolutions by acquiring the smallest amount of information required and/or in several acquisitions synchronized by the electrocardiogram (ECG).[39] In addition, 3D transducers allow the acquisition of up to three simultaneous two-dimensional images of different planes, which are very useful in the evaluation of LVOT, AV, and Ao[39] (Fig. 26). Detection of complex plaques in Ao is of great clinical importance due to the association between them and the risk of embolization and mortality in patients undergoing cardiothoracic surgery.[40–42] As described previously, the use of Ao simultaneous biplanar images allows to save time and gain precision in the evaluation of atherosclerotic plaques (Fig. 27).[41] Once identified, these plaques should also be evaluated on 3D mode, which adds diagnostic quality and sensitivity to this investigation, reason why it is the method of choice for aortic atherosclerotic plaques evaluation.[43] All these technical advantages are applied for detailed evaluation of aortic syndromes, such as aortic dissection, in which the 3D exam provides additional information, particularly in the quantification of the inflow orifice, in addition to allowing a better morphological understanding when the intimal dissection occurs in a spiral.[44] The increased information on diagnostic evaluation is repeated in therapeutic procedures, when it becomes a valuable intraoperative tool to improve the operator's work, during and after the positioning of Ao thoracic stents.[45] With the exponential expansion of the percutaneous treatments of AV pathologies, there was a great interest in the precise anatomical definition of LVOT and AV, through the evaluation of the shape and measurements of diameters, area and planimetric perimeters. This definition influences influence

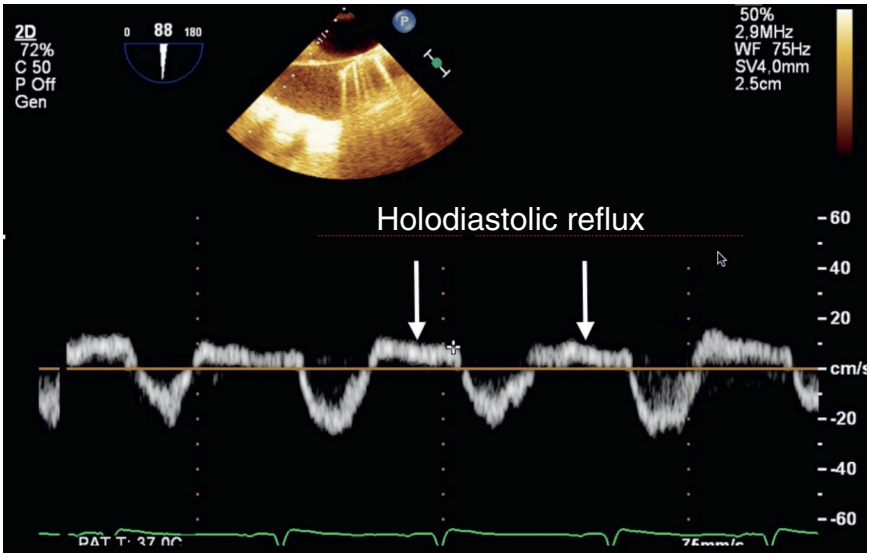

Figure 23 Pulsed Doppler in descending aorta showing a holodiastolic reflux of severe aortic regurgitation.

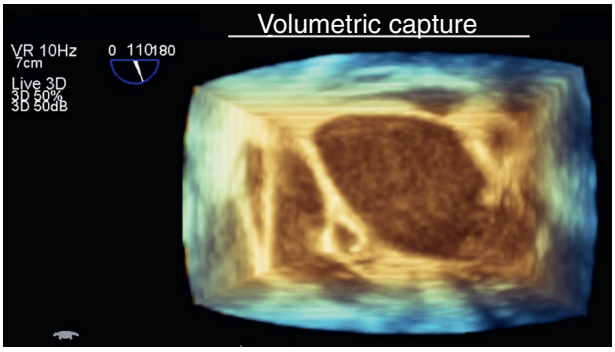

Figure 24 Three-dimensional volumetric analysis of aortic valve.

the outcome of these procedures, as far as two-year mortality is concerned,[46,47] and could only be measured with 3D images (Fig. 26), since calculations using the mathematical formulas of 2D echocardiography were shown to be significantly inaccurate.[26,48] The identification that LVOT has an elliptical shape in most patients increased the importance of 3D TEE due to the inability of 2D echocardiography to perform these important measurements accurately.[26] The distant location from the transducer focus, the distal curvature, the thin thickness of the AV valves, and the artifacts resulting from the reverberation and acoustic shadow of the existing calcifications are some of the challenges for the acquisition of 3D echocardiographic imaging of the aortic root.[26] Color Doppler 3D should also be used to evaluate normal flow and abnormalities, allow two-dimensional cuts with perfect spatial orientation, and the odd analysis of all abnormal flow aspects, such as measurement of the contracted vein area, which is important to quantify these flows, without the need to apply geometric formulas that are imprecise for the situation.[37]

Pulmonary valve

Anatomy

PV is a thoracic anterior structure located obliquely to the plane of the AV.[49] It is a semilunar valve comprising three valves denominated by their positions relative to the AV (left, right, and anterior).[49] Unlike PV, there is no continuity of PV with the cardiac fibrous skeleton or right atrioventricular valve.[49] Because its valves are thin and poorly echogenic and because it is far from the transesophageal probe, PV evaluation using TEE is generally difficult.[1]

2D and Doppler modes

RVOT, PV, and pulmonary artery dimensions are best evaluated through the cross-sectional view of the mid-esophageal RV inflow and outflow tracts, in which the US beam is perpendicular to these structures (Fig. 5B).[49] The anterior valve in this cross-section is the one furthest from the transducer, whereas the one closest to the AV may correspond to the right or left valve. In cases where these sectional view is of poor quality, TG cross-sections of the RV inflow and outflow tracts, upper esophageal aortic arch short axis (Fig. 9B), and mid-esophageal Asc Ao short and long axes (Fig. 4C and D) may be used to supplement information on structure, dimensions, and function of the pulmonary valve and artery.[1]

The presence of regurgitation or flow acceleration can be assessed by color Doppler mode in the mid-esophageal RV inflow and outflow tracts view. For transpulmonary flow evaluation (pulsed and continuous Doppler modes), the US bundle good alignment can be obtained in cross-sectional views of the mid-esophageal Asc Ao long axis and, alternatively, the upper esophageal aortic arch short axis, transgastric RV inflow and outflow tracts, and transgastric basal short axis.[1,50]

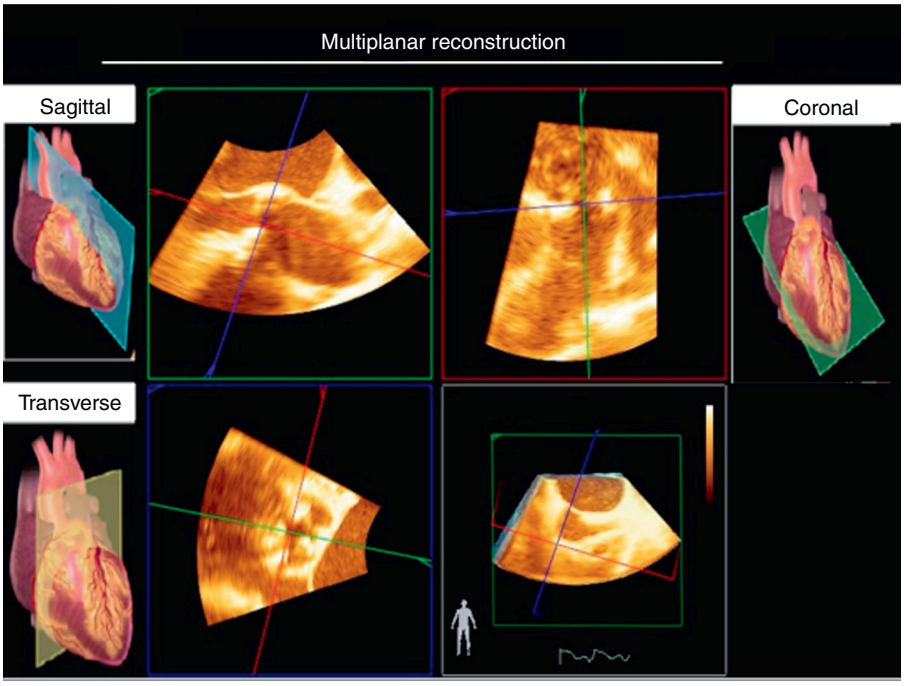

Figure 25 Three-dimensional multiplanar reconstruction of aortic valve.

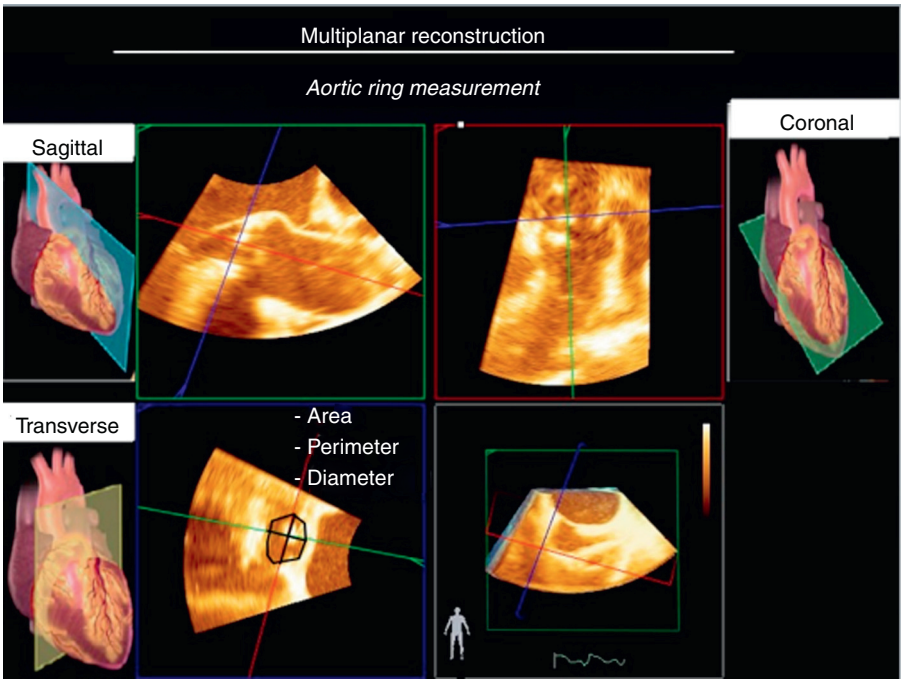

Figure 26 Multiplanar reconstruction in assessing aortic valve area.

3D pulmonary valve

PV 3D images can be acquired on upper esophageal aortic arch short axis or mid-esophageal aortic valve long axis cross-sections after a slight rotation of the probe to the left.[1,49]

By allowing the simultaneous view of two planes, modern 3D probes enabled the assessment of PV in its short axis. For this purpose, the cross-sectional view of the mid-esophageal RV inflow and outflow tracts is obtained and an orthogonal plane is positioned over the PV.[1]

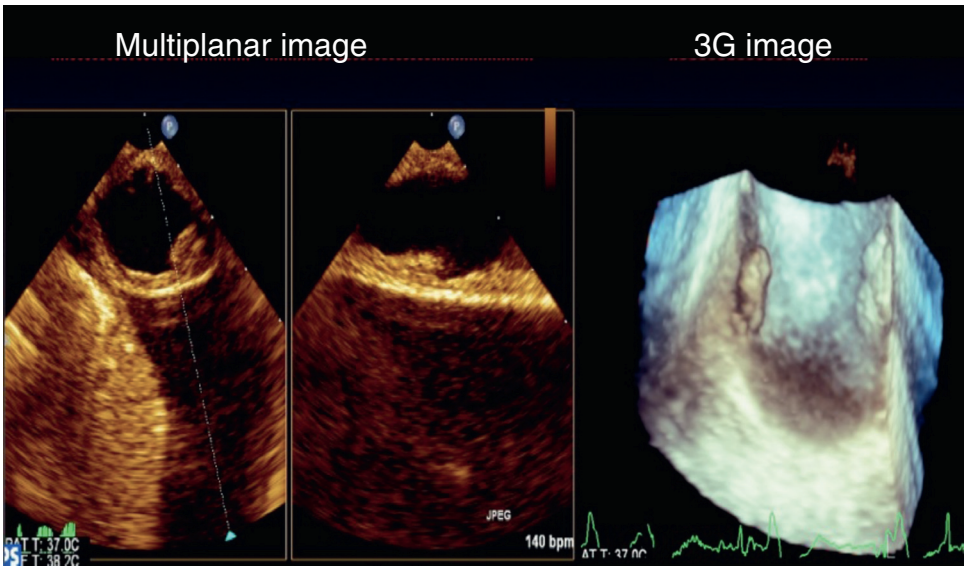

Figure 27 Three-dimensional image of descending aorta atherosclerotic plaque.

Left atrium and pulmonary veins

Anatomy

In relation to the rib cage, the LA is the most posterior chamber of the heart. It is located very close to the esophagus, separated only by the fibrous pericardium.[51] Trachea bifurcation, esophagus, and Desc Ao are immediately behind the LA posterior wall. This LA proximity to the esophagus is very advantageous for TEE, as LA is used as a window to obtain the mid-transesophageal views.[1,51] In these views, LA is always at the top of the screen, close to the US beam (Fig. 1).[1] In relation to RA, LA is more posterior and superior and is separated from RA by IAS.[52]

LA walls can be described as superior, posterior, left lateral, septal (or medial), posterior–inferior, and anterior.[53] LA anterior wall is behind the transverse sinus, that is, behind the Ao root. CS goes through the posterior–inferior wall of the LA. LA walls are muscular and its thickness may vary from 1 ± 0.5 mm. Abnormal wall thickening may indicate the presence of a mural thrombus or even endocarditis. Mitral annulus calcification may extend to the LA wall and make it thicker.[1,52]

LAA is a blind bottom structure with an aperture to LA. In relation to LA, it is located lateral and superior and its tip is directed anteriorly, overlaps pulmonary artery trunk and left coronary artery.[51] LAA has an average diameter of 10–24 mm, but this value may vary. Compared to RAA, LAA has a narrower orifice that facilitates the formation of thrombi in situations of low blood flow and in non-sinus cardiac rhythms.[51] Between LAA and ULPV there is a triangular fold of the serous pericardium called coumadin ridge, which when prominent may be confused with thrombus or atrial mass (Fig. 6B).

According to the blood flow, LA starts at the venoatrial junction and ends at the MV orifice. The four pulmonary veins enter the posterior part of the LA, the left veins are located more superior than the right veins.[51] There are two right (RUPV and RLPV) and two left pulmonary veins (LUPV and LLPV). The RUPV passes behind the RA junction with SVC and the RLPV passes behind the intercaval area.[52] The right pulmonary veins orifices are directly adjacent to the IAS plane. On the other hand, the left pulmonary veins are located between LAA and Desc Ao, ULPV is positioned posteriorly superior to the IAS, whereas LLPV is positioned posteriorly inferior.[52,54]

Physiology

LA is not just a simple blood-carrying camera. It responds dynamically to its distention with the secretion of atrial natriuretic peptides and participates in the management of body fluids.[55] LA also functions as a blood reservoir from the pulmonary veins during ventricular systole and isovolumetric relaxation. During diastole, LA works as blood conduit to LV. At the end of diastole, atrial systole occurs, contributing with 15–30% of the volume transferred to LV.[56] Because LA is an LV continuum during diastole, changes in ventricular compliance affects the size and function of LA.[56,57]

The increase in LA is a predictor of cardiovascular adverse events, as well as the onset of atrial fibrillation, intracardiac thrombi formation, and cerebrovascular accidents (Fig. 28A and B).[58] When a thromboembolic source is investigated, LAA is the first site to be evaluated; TEE has a sensitivity and specificity for thrombus diagnosis of 100% and 99%, respectively. However, because they are small and complex structures, they can be left undiagnosed in some circumstances.[59]

2D and Doppler imaging of left atrium and left atrial appendage

The most frequently used cross-sections for LA evaluation are[1]:

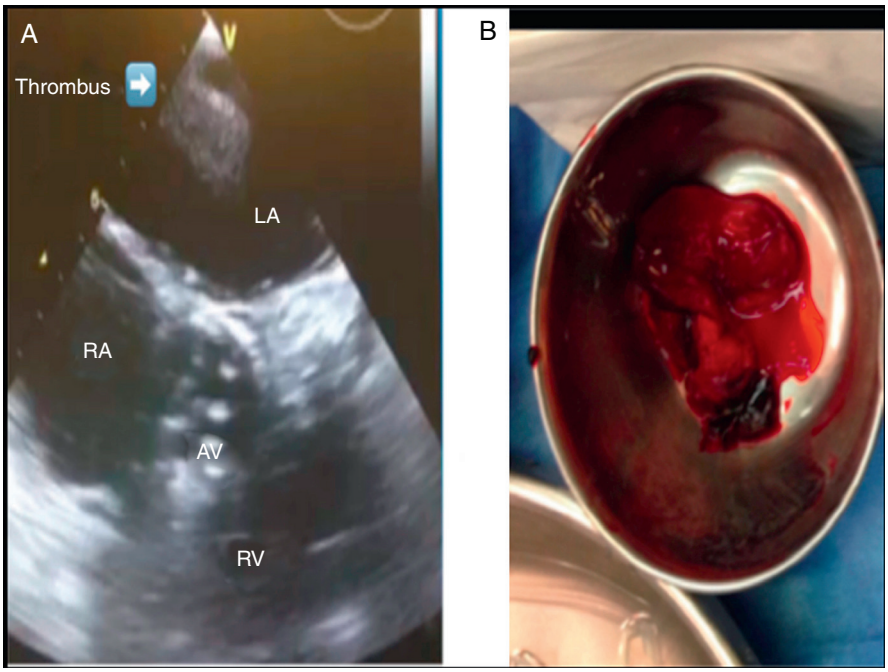

Figure 28 (A) Echocardiographic image of left atrium thrombus. (B) Thrombus. LA, left atrium; RA, right atrium; AV, aortic valve; RV, right ventricle.

- Mid-esophageal four-chamber (Fig. 3B);
- Mid-esophageal commissural (Fig. 3C);
- Mid-esophageal two-chamber (Fig. 3D);
- Mid-esophageal left atrial appendage (Fig. 6B);
- Mid-esophageal long axis (Fig. 4A);
- Mid-esophageal aortic valve short axis (Fig. 5A);
- Mid-esophageal bicaval (Fig. 5D);
- Transgastric two-chamber (Fig. 8A);
- Deep transgastric (Fig. 7D).

The cross-sectional images that most easily evaluate the LA are the mid-esophageal ones. LA is the structure closest to the US bundle in the mid-esophageal views; it is always found at the top of the screen. TEE cross-sections that evaluate MV will necessarily evaluate LA.[1]

LA evaluation starts from the mid-esophageal four-chamber view (Fig. 3B). Rotate the angle, going through the other views to obtain 2D cross-sections. In two-chamber view (Fig. 3D), LAA image should be increased (Fig. 6B) to better visualize the presence of thrombi, particularly in risk patients. In bicaval view, the relationship between LA and IAS and RA is evaluated, looking for PFO and IAS defects. In these cross-sections, the pulmonary veins will also be evaluated, as will be discussed below. After the esophageal evaluation, the transducer is advanced to the TG cross-sections. At the 90° angle, LA and especially MV and its subvalvar apparatus are evaluated. In deep TG cross-section (Fig. 7D), LA can also be visualized, but this view is more used for transaortic flow evaluation; LA is a secondary evaluation because it is further away from the US beam, with a lower resolution compared to transesophageal cross-sections.

Due to the proximity between LA and esophageal transducer, LA cannot be evaluated in its entirety by a single view, which makes its complete evaluation and its diameter and volume measurements difficult on TEE.[1] LA area and volume may be underestimated. The linear measurements acquired on TEE in mid-esophageal aortic valve long and short axes views are the ones that best correlate with the TEE parasternal long axis cross-sectional measurement, which measures LA in the anterior-posterior sense.[60] In longitudinal sense, the vertex should be measured from sector to Ao root, but these measurements have no normalized values. Septolateral measurements and LA volume can be obtained with mid-esophageal four- and two-chamber cross-sections. However, these measurements, although correlated with those obtained on TEE, have no normalized values.[60]

LAA evaluation may be initiated with the four-chamber cross-section, but because it is a lateral structure, the probe should be rotated counterclockwise and anteflex to bring LAA to the screen center.[1] Also in the two-chamber cross-section, LAA site can be zoomed in or the screen depth be reduced to evaluate LAA more accurately. An organized thrombus is echocardiographically defined as a well-circumscribed mass of uniform consistency and a texture different from that of the atrial wall (Fig. 28).[1] Spontaneous contrast is not well circumscribed, has a dynamic localization, and appears as a ''cigarette smoke'' – this image is caused by the slowing down of blood flow (Fig. 29).[61] In high-risk patients for LAA thrombus (atrial fibrillation), the risk of thrombus formation should be assessed through the analysis of blood flow velocity.[61] Pulmonary Doppler should be placed 1–2 cm from LAA ostium. Velocities lower than 27 $cm.s^{-1}$ are associated with the formation of spontaneous contrast, thrombus, and embolic events.[62]

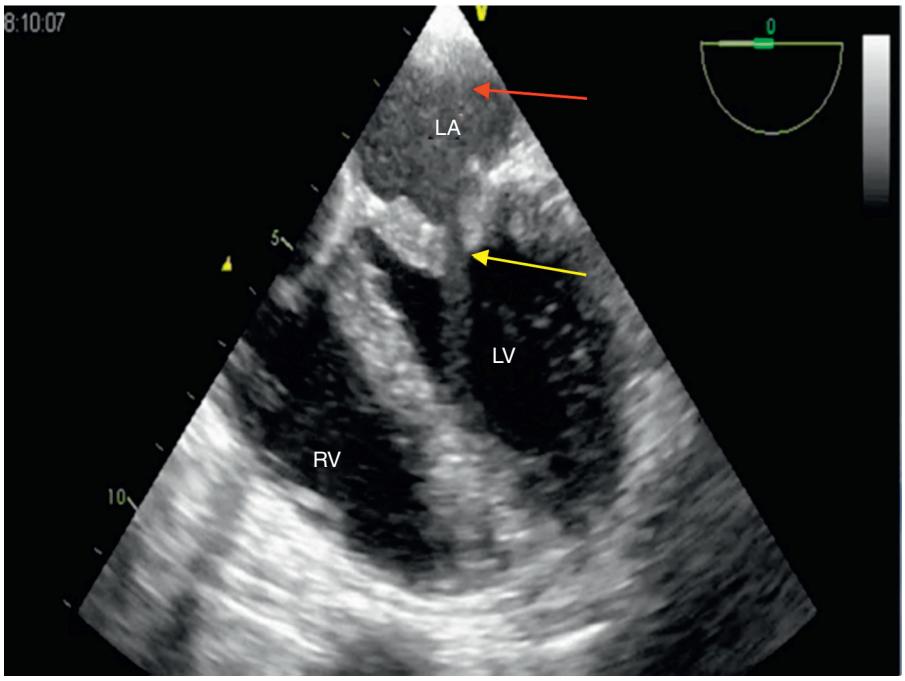

Figure 29 Mid-esophageal four-chamber cross-section showing rheumatic mitral stenosis. Note the presence of spontaneous contrast in left atrium and mitral valve leaflets thickening. LA, left atrium; LV, left ventricle; RV, right ventricle. *Source*: Personal collection. Yellow arrow indicates mitral stenosis. Red arrow indicates ''cigarette smoke'' in left atrium.

2D and Doppler imaging of pulmonary veins

ULPV is the most easily found by TEE. When LAA is found in the 60° mid-esophageal plane, the probe is gently removed and ULPV will appear above and posterolateral to LAA and to the coumadin ridge (anatomic variant that is occasionally found in the left atrium) (Fig. 6A).[1]

The LLPV is the most difficult pulmonary vein to obtain on TEE image. After the ULPV image is obtained, the angle is increased to 90°. The left pulmonary veins will appear as an inverted V-shape. Colored Doppler is set to a velocity of 40 $cm.s^{-1}$ and laminar blood flow is observed toward the TEE transducer. Another way to acquire the LLPV image is, after finding LAA, advance the probe and rotate it slightly clockwise and when LAA has disappeared, LLPV will be visible.[1]

RUPV is found with the mid-esophageal bicaval cross-section at 110–120°, near the right pulmonary artery.[63] The angulation is returned to 90°, and the two right pulmonary veins in inverted Y-shape can be evaluated. The right pulmonary veins can be visualized at zero degree mid-esophageal by rotating the probe to the right so that the right side of LA lies in the central part of the screen. From this position, the angle is opened to 30° and RUPV is located to the right of the screen and RLPV to the left of the screen, entering perpendicular to LA.[63]

To assess the blood flow pattern of pulmonary veins, apply pulsed Doppler with a velocity limit of 40 $cm.s^{-1}$. The normal flow pattern is three-phase with systolic (S1 and S2), diastolic (D), and reverse atrial (A) waves. Diastolic dysfunction, mitral diseases, and rhythm disturbances change this normal pattern.[1]

Right atrium, tricuspid valve and venous connections

RA is the heart cavity that receives systemic venous blood from IVC and SVC, as well as blood returning from the coronary arteries through CS. Its medial and posterior wall is the IAS, the structure that separates it from LA. Its floor is the TV, which opens into the right ventricle.[64] Seen from the right side, IAS has a characteristic structure, an oval fossa, which shows outward contour and central region constituted by a delicate blade. This blade most anterior portion may not be completely adhered to the oval fossa edge, the so called PFO.[65] Necropsy studies suggest that it is present in up to 27% of adults. Its in vivo diagnosis depends on dynamic evaluation with maneuvers that cause increased RA pressure concomitant with the injection of agitated saline solution. A higher prevalence has also been associated with the presence of IAS aneurysm.[65]

The LA lower portion is separated from LV by a portion of fibrous tissue that continues with IVS, called fibrous septum. This is due to the different levels of implantation of the tricuspid and mitral valves. TV has more apical insertion, which results in the area known as atrioventricular septum.

CS outflow is located posteriorly and medially to the IVC ouflow next to the atrioventricular transition. In this region, remnants of venous valves may be found, with the Eustachian next to IVC and the Thebesian related to CS.[64]

RA also has two important structures for cardiac automatism: sinus node and atrioventricular (AV) node. The sinus node is located near the SVC outflow, while the AV node is close to TV. TV consists of fibrous annulus, *chordae tendineae*, papillary muscles, and three leaflets.[1]

RAA is an atrial cavity projection, shaped like a ''glove finger'', covering the AV groove on the right (Fig. 5C). The inner RAA surface has parallel muscle ridges, which extend posteriorly, named pectinate muscles, ending in a transverse muscle band rather prominent named terminal ridge.[66]

2D echocardiography and Doppler assessment

Starting with the mid-esophageal four-chamber plane (Fig. 3B), the general aspect of RA can be assessed, its size relationship with the other cardiac chambers, as well as the mid-anterior and inferior portions of IAS, corresponding to the oval fossa and septum primum region.[1]

From this position, the transducer is lowered toward the TG planes, and the angle is maintained at zero degree, eventually a slight retroflection of the probe is performed, and a longitudinal image of the CS is acquired, a lower and posterior structure.[1]

Occasionally, CS can be assessed from the mid-esophageal bicaval plane (Fig. 5D), with a discreet advancement and turning the probe clockwise. Still in the bicaval plane (Fig. 5D), SVC, IVC, Eustachian valve, terminal crest, and RAA are identified. From this view, the oval fossa is also well defined, as well as a PFO eventual blade. A discreet movement of the probe toward the upper esophagus allows a more complete picture of SVC. At this point, rotate the probe clockwise and the right upper and lower pulmonary veins will be visualized. Thus, the suspicion of anomalous drainage of these veins is typically investigated from this point of view.[1]

By introducing the probe toward the TG planes from the bicaval plane and maintaining the angle at 90°, IVC and Eustachian valve can evaluated. Moreover, this position may be useful to evaluate the image of hepatic veins and their possible inadvertent cannulation during cardiopulmonary bypass.[1]

Interatrial shunt diagnosis

In suspected cases of atrial septal defect, a complete examination should include a comprehensive assessment of IAS in 2D mode and color Doppler, as defects may occur in any location.[67]

Assessment of left ventricular size and function

The evaluation of LV size and function is an important component of any perioperative echocardiographic exam.[68] The degree of ventricular systolic dysfunction besides being a strong predictor of clinical outcome aids in the stratification of surgical risk and therapeutic interventions.[68] Echocardiography provides a global and segmental assessment of ventricular performance through analysis of systolic thickening, ventricular size and volume.[69] Qualitative and quantitative measures to estimate ventricular function can be made through 2D, 3D, application of Doppler and by measurements of myocardial velocity and deformation.[69]

Anatomy

LV is a thick wall cavity with a conical shape, which decreases in diameter from the base to the apex, appears as a circular structure in the transverse plane. Through this same plan the IVS myocardium follows the LV shape and is part of it from the anatomical and functional point of view.[70] In order to facilitate an accurate description of the location and severity of LV segmental changes, besides allowing a standardized communication of echocardiography with other cardiovascular imaging methods, LV is divided into 17 segments.[70] In this model, LV is divided into three levels: basal, at the mitral valve level (six segments); medial, at the papillary muscle level (six segments); and apical, after insertion of papillary nerves up to the end of the cavity (four segments), with the 17th segment located at the tip of LV.[30] The TEE cross-sectional image recommended for measurement of LV diameters are the mid-esophageal two-chamber and long axis and the TG two-chamber. Measurement is done from the endocardium of the anterior wall to the endocardium of the inferior wall, between the basal and medial third of the ventricle. The proposed view to measure the left ventricular wall thickness is the TG mid-short axis[30] (Fig. 30).

2D and 3D imaging of left ventricle

The assessment of left ventricular function and structure with 2D echocardiography uses five main cross-sections from mid-esophageal and TG planes, which are: mid-esophageal four-chamber, mid-esophageal two-chamber, mid-esophageal longitudinal, TG mid-short axis, and TG longitudinal.[1,2] The most used cross-section for LV segmental changes monitoring is the TG mid-short axis, in which we can visualize the territories irrigated by the three main coronary arteries[2,6] (Fig. 31). The analysis of LV segmental function is based on the visual qualitative evaluation of parietal motion and systolic thickening. Ideally, the function of each segment should be assessed through multiple incidences.[71] LV parietal motion follows this recommendation: normal segments, hypokinetic segments (mild to moderate thickening), akinetic segments (without thickening), and dyskinetic segments (paradoxical systolic motion).[2] Despite the absence of reference values and reproducibility below ideal, the quantitative evaluation of the regional LV strain magnitude is promising, mainly through the longitudinal strain during ventricular systole.[71]

In order to improve the image quality for ventricular function correct quantification and interpretation, some technical considerations must be observed: correct image depth adjustment to include the entire LV; avoid apical region shortening through proper manipulation of the probe (anteflexion and retroflexion); correct identification of the end of systole and diastole (check the motion of mitral and aortic valves, the largest and smallest cavity size and ECG signal); correct Doppler alignment with the direction of blood flow; appropriate gain and focus adjustment to improve endocardium visualization; and use of second harmonic image.[72]

Perhaps one of the most valuable perioperative contributions of 3D echocardiography is related to the quantification

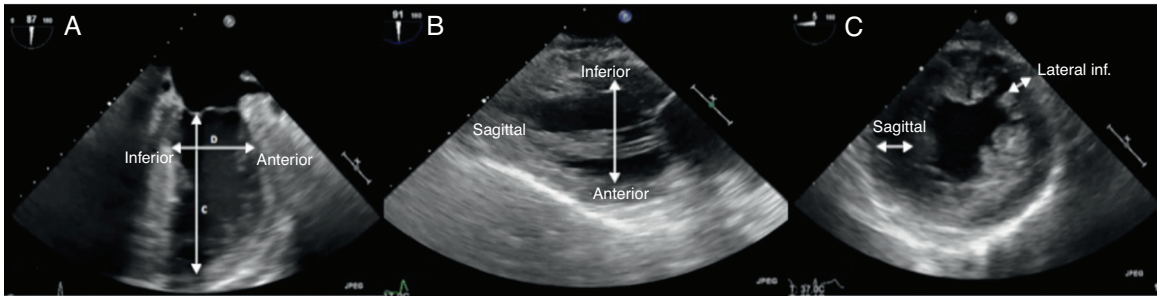

Figure 30 Transgastric cross-sections for left ventricle assessment. (A) Mid-esophageal two-chamber view. (B) Transgastric two-chamber view. (C) Transgastric mid-papillary short axis view.

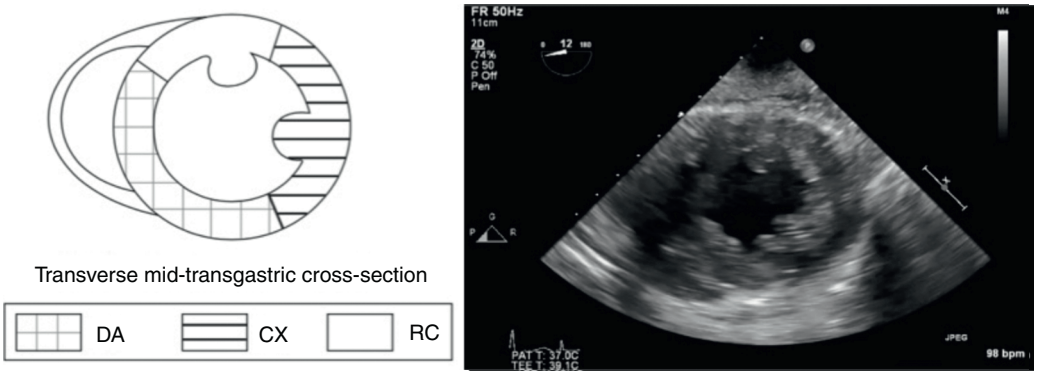

Figure 31 Anatomic relationship and coronary irrigation with left ventricle walls in transgastric cross-section. DA, anterior descending coronary artery; CX, circumflex coronary artery; RC, right coronary artery. Adapted from Galhardo et al.[6]

of left ventricular volume and function.[7] Ventricular function analysis consists of using a software capable of semi-automatically detect the endocardial edge and make more accurate volumetric calculations, which allows an accurate analysis of global and segmental LV function measurements, irrespective of the ventricle geometric shape and with better measurement replication among examiners.[70,73]

Quantification of global LV systolic function

One of the most routinely used methods in the operating room for global LV function quantification is qualitative or semi-quantitative, through which a visual estimation of the ventricular ejection fraction is made after the evaluation of multiple orthogonal cuts. This method has an acceptable correlation compared to quantitative measurements.[74]

Quantitatively, the systolic ventricular function estimation is evaluated by parameters that measure the difference between the final diastolic and systolic values related to left ventricular cavity dimension and volumes. Among the quantitative methods, the most used in clinical practice have focused on measuring cardiac output, ejection fraction, shortening fraction, fractional area change, ventricular performance index (Tei index),[75,76] and on methods that evaluate the velocity and range of myocardial motion and deformation (tissue Doppler, strain and strain rate).[3,77]

Ventricular function assessment limitations

The patient's overall hemodynamic condition should be taken into consideration during ventricular function assessment because changes in blood volume and use of anesthetic drugs may affect systolic function by its effects on pre- and post-load. Moreover, other factors that may compromise the TEE function evaluation are related to LV tip shortening and exclusion in the evaluation of global and segmental contractility and difficulties in correctly aligning Doppler to blood flow, which interferes directly in the calculation of ventricular ejection rates.[1]

Right ventricle

Anatomy systolic evaluation indexes

RV is a tubular V-shaped or ''bagpipe'' chamber, with tricuspid ring and pulmonary ring forming this V tips. The free, septal, and apical walls delineate the anterior, posterior, and inferior margins. RV anatomical divisions are the inflow, body, and outflow regions. The free wall is subdivided into inferior, anterior, and lateral segments, based on echocardiographic incidences. RV irregular shape makes it difficult to evaluate systolic volume and function with simple uniplanar and geometric methods. Moreover, the RV trabecular interior also creates problems in defining the endocardial border.[1]

Echocardiographic evaluation

Systolic evaluation indexes:

- Geometric indexes: reflect the extent of contraction, such as fractional area variation, ejection fraction, and tricuspid annular plane systolic excursion (TAPSE) (Fig. 32);
- Velocity indexes: isovolemic acceleration (Fig. 33);
- Hemodynamic indexes: right ventricle dp/dt;
- Time interval indexes: such as myocardial performance index or Tei index (Fig. 34).

The main incidences for RV visualization with TEE are:

- Mid-esophageal four-chamber (Fig. 3B): to visualize the free wall, IVS, IAS, and TV (anterior and septal leaflets);
- Mid-esophageal RV inflow and outflow (Fig. 5B): VT, VSVD and VP;
- Mid-esophageal bicaval (Fig. 5D): RA, RAA, IAS, cava veins, and TV;
- Transgastric short axis: face view of TV, IVS, and free wall;
- Transgastric right ventricle inflow: free wall, TV, and subvalvar apparatus;
- Deep transgastric (Fig. 7D): TV, RVOT, and PV.

Left ventricular diastolic performance

Diastole is no longer considered a passive LV filling period but an important complex period, which depends on adequate ventricular relaxation, compliance and systolic function, intrathoracic pressure, ventricular interaction, cardiac rhythm, and atrial function.[78]

In the general population, the asymptomatic prevalence of diastolic dysfunction is approximately 30% in individuals older than 45 years. In surgical patients over 65 years of age, the prevalence of diastolic dysfunction with normal ejection fraction rises to about 60%.[78] In patients undergoing large vascular surgery, the isolated diastolic dysfunction is associated with an increase in 30-day cardiovascular events and long-term mortality. relationship between dysfunction severity and reduced survival In cardiac surgery, diastolic dysfunction is associated with difficult cardiopulmonary bypass weaning, increased need for inotropic support, and increased morbidity.[79] In a study published in 2014, Nicoara et al.[80] correlated the degree of diastolic dysfunction with survival after surgical procedures and showed a relationship between dysfunction severity and reduced survival.

Diastolic dysfunction is a finding that appears concurrently with a number of cardiovascular diseases, ranging from arterial hypertension to infiltrative diseases such as amyloidosis.[80] Heart failure due to diastolic dysfunction is being increasingly diagnosed (about 50% of patients with congestive heart failure have diastolic dysfunction and normal ejection fraction).[81] Diastolic function assessment allows the anesthesiologist to detect increases in left ventricular end-diastolic pressure in the absence of a pulmonary artery catheter.[82] Diastolic dysfunction precedes systolic dysfunction in cases of acute ischemia and during the perioperative period; diastolic function assessment may help to guide therapy, with the use of vasodilator drugs rather than inotropic drugs.[80]

Echocardiography is the safest modality with high sensitivity and specificity to evaluate diastolic function and identify other associated abnormalities.[83] Assessment should be performed at mid-esophageal level, where the best alignment between mitral flow and US bundle is obtained.

Diastole is divided into four phases. The first phase begins with the AV closure and ends with the MV opening, lasting between 90 and 120 ms. As both VA and MV are closed, this period is called the isovolumetric relaxation time (IVR). When the left ventricular pressure falls below the left atrial pressure, the MV opens and the second phase of the diastole begins, that is, the rapid ventricular filling, which corresponds to 80% of the ventricular filling. LV pressure increases during rapid filling and the pressure gradient between LV and LA decreases progressively. This reduction in pressure gradient delays ventricular filling and diastasis occurs, a period of pressure equalization until the beginning of the atrial contraction and which accounts for 5% of the volume. This period increases when there is reduced LV relaxation and decreases when ventricular compliance is decreased. Finally, atrial contraction occurs, contributing with only 20% of the ventricular filling, but in cases of diastolic dysfunction, especially in elderly patients, it may account for 50% of the filling volume.[79]

If we correlate the above periods of mitral diastolic flow pattern with pulsatile Doppler, we have: (a) isovolumetric relaxation period, time between LVOT and mitral flow (this period increases when there is compromised relaxation and decreases when left atrial pressure increases); (b) fast ventricular filling phase, represented by the E wave; (c) deceleration time (DT), which represents the time required for the pressure to drop from the E wave peak to baseline[79]; (d) atrial contraction phase, responsible for the diastole fourth phase. This phase is also termed late ventricular filling and is represented by the A wave.[79]

It should be borne in mind that mitral flow velocities recorded by Doppler are determined by the transmitral pressure gradient, which depends on several variables: rhythm, early filling loads, atrial contractility, MV disease, ventricular septal interactions, LV intrinsic lusitropic state, ventricular relaxation and compliance.[79] In this sense, the maximal velocity of the mitral E wave is an indirect measure of left atrial pressure. E wave velocity correlates with the difference between left atrial and left ventricular pressures at the time of mitral opening. Thus, the higher the left atrial pressure (or the higher the preload) at the time of MV opening, the higher the E wave velocity.[79]

The relationship between the velocities of E and A waves must be greater than 1 (Fig. 35A). Normally, this relationship is expressed as $E/A > 1$. When $E < A$, it can be said that there is an impairment of left ventricular relaxation (Fig. 35B). On the other hand, E wave greater than double the size of A wave represents a restrictive pattern; that is, LV compliance is compromised (Fig. 35C). There may however be a time when LV has a diastolic dysfunction in transition; the mitral flow pattern passes from a predominance of relaxation change to a predominance of compliance change. In this case, the E/A relationship is similar to the normal pattern ($E > A$). This pattern, termed pseudonormal, represents a moderate stage of diastolic dysfunction, in which an earlier, near-normal transmitral pressure gradient is

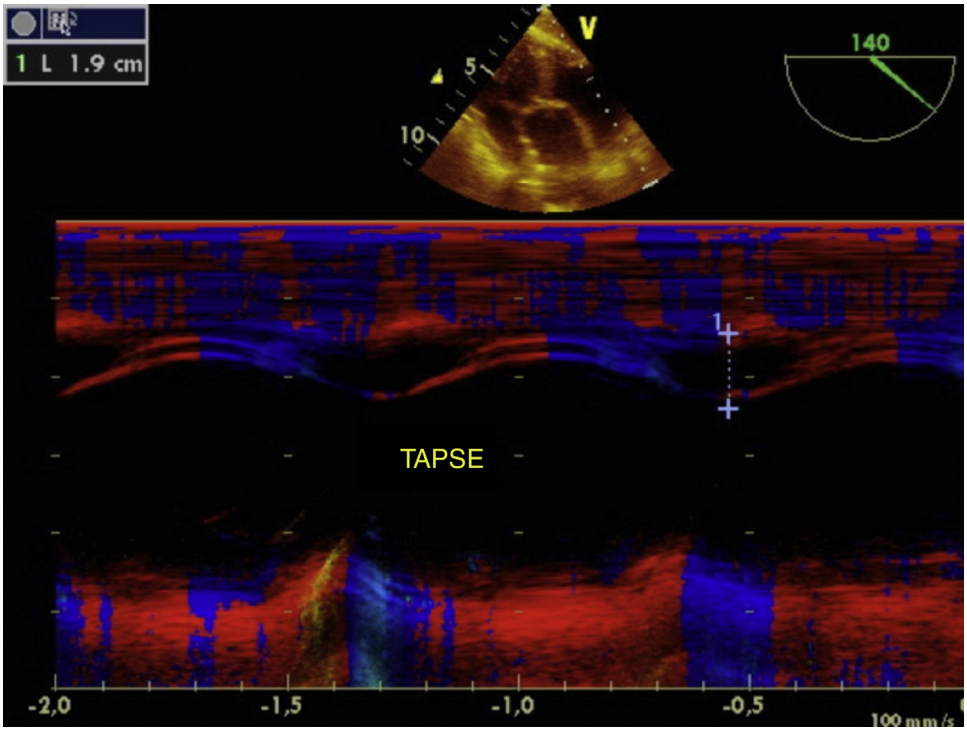

Figure 32 Tricuspid annular plane systolic excursion (TAPSE) is acquired by placing the M mode on tricuspid annulus and measuring the longitudinal systolic motion amplitude. Transesophageal echo transducer should be positioned in mid-esophageal four-chamber and RV centralized.[3,5,6] In a minority of patients, a modified incidence of RV deep transgastric can be obtained by rotating the probe to the right (as in the figure), which allows US good alignment with tricuspid ring motion.

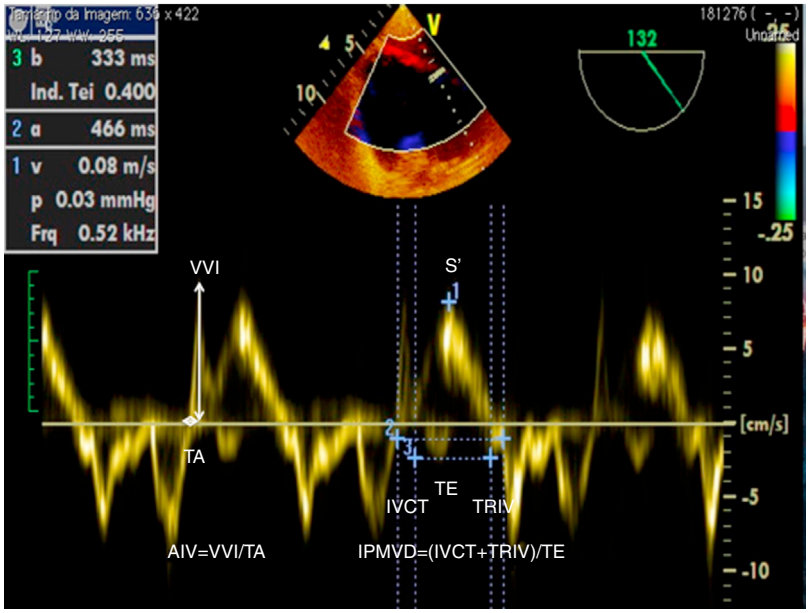

Figure 33 Tissue Doppler image of tricuspid ring: S′, right ventricular longitudinal peak velocity; IPMVD, right ventricular myocardial performance index or Tei index; TRIV, isovolemic relaxation time; AIV, isovolemic acceleration; TA, acceleration time; TE, ejection time; IVCT, isovolemic contraction time; VVI, isovolemic peak velocity. Isovolemic acceleration is a systolic performance index relatively independent on pre- and post-load. More information about its use in cardiac surgery is required.

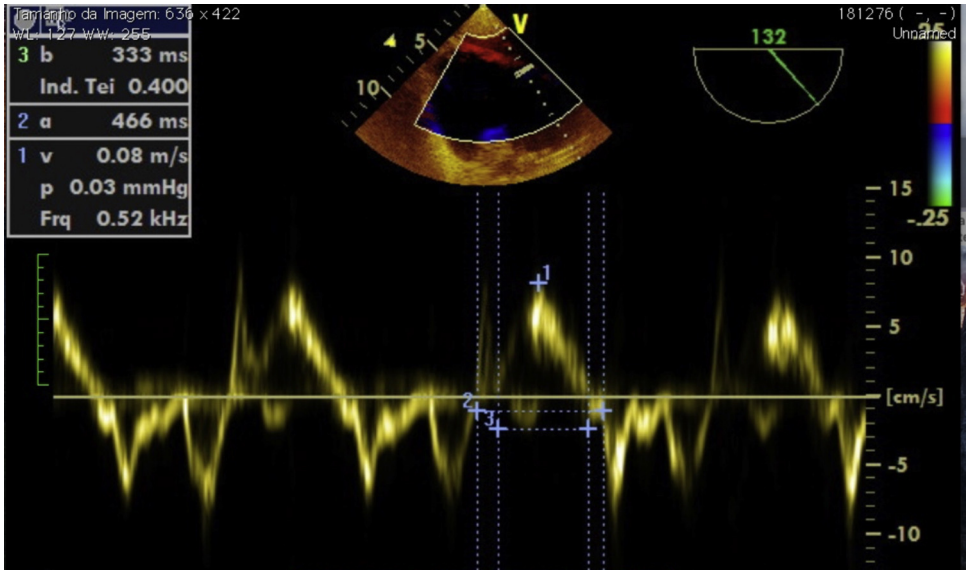

Figure 34 Right ventricular myocardial performance index (RMPI) or Tei index. This figure shows the tissue Doppler of tricuspid ring in deep transgastric right ventricular view.

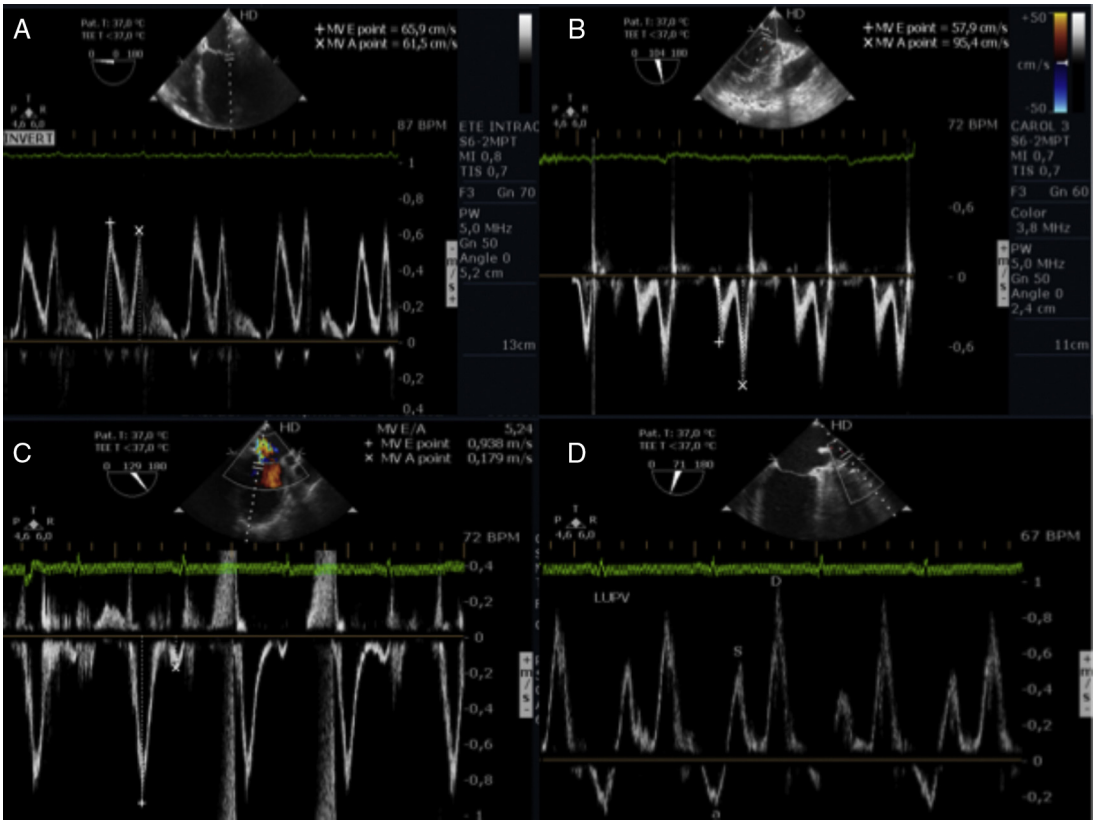

Figure 35 (A) Trasmitral pulsed Doppler, E wave > A wave. (B) Trasmitral pulsed Doppler, E wave < A wave. (C) Trasmitral pulsed Doppler, E wave > A wave. (D) Pulmonary Doppler on pulmonary vein, S wave < D wave.

generated by the balance between the impaired LV relaxation and the gradually increasing LV pressures, as compliance decreases.[79]

In order to differentiate a normal from pseudonormal pattern, mitral annular tissue Doppler (mitral TDI) and pulmonary veins Doppler flow pattern are used (Fig. 35D).[79] The analysis of mitral TDI helps to differentiate a normal pattern from a pseudonormal because the wave that coincides with the rapid ventricular filling (represented as E′ or Ea) remains reduced with pseudo-normalization. This

approach is based on the Doppler technique to measure mitral annular velocity in diastole. A small volume sample should be used and the gain and filter should be set downward. This velocity profile seems to be more dependent on left ventricular relaxation and less dependent on transmitral pressure gradient. Thus, the E′ wave assessment is a measurement relatively insensitive to LV preload and may be useful intraoperatively when the loading conditions may vary considerably.[79]

As diastolic dysfunction progresses, the E′ wave tends to decrease and the mitral E wave tends to increase, due to the compensatory increase in left atrial pressure that accompanies the impaired relaxation. Thus, an E/E′ ratio <10 is considered normal, while an E/E′ ratio >15 predicts a left ventricular filling pressure above 15 mmHg.[78,79]

The flow pattern of pulmonary veins also has a systolic and a diastolic component. The systolic component can be divided in two: a first time when the flow accompanies the atrial relaxation and a second time that accompanies the mitral annulus displacement toward the left ventricular apex. The diastolic component occurs when the MV opens. At the end of diastole, simultaneously with the atrial contraction, a reverse flow is observed, representing blood from the LA toward the pulmonary veins. This reverse flow assessment is also important for diastolic function evaluation: an increased retrograde flow reflects an increased LV end-diastolic pressure.[79,84] Table 3 shows the patterns of diastolic function schematically.[79]

Another parameter that may be used in diastolic function assessment is the propagation velocity (Vp) of transmitral flow within LV in color M mode. It has the advantage of being relatively independent of preload. This parameter reflects the effectiveness of LV suction at the onset of diastole. Values below 50 $cm.s^{-1}$ are consistent with impairment of ventricular relaxation (Fig. 36).[79,80] Recent studies show that Vp lower than 40 $cm.s^{-1}$ may be a predictor of required cardiovascular support after aortic valve replacement due to stenosis. In addition, Vp may be useful in estimating filling pressures, as an E/Vp ratio greater than 2.5 predicts a pulmonary capillary occlusion pressure greater than 15 mmHg.[79,80]

It is important to emphasize that diastolic function evaluation is subject to functional changes in MV itself, such as stenosis and insufficiency. Because much of the diastole interpretation is based on transmitral flow, the diastolic function assessment is impaired in patients with mitral valvopathy.

Patients with arrhythmias should also have diastolic function evaluated carefully, as transmitral flow is affected by heart rate and rhythm. Sinus tachycardia and first-degree atrioventricular blockade may lead to fusion of E and A waves, hampering the visualization of both, as

Table 3 Classification of diastolic dysfunction.

Pattern	Normal	Relaxation deficit	Pseudo-normal	Restrictive
IVRT	70–90 ms	> 90 ms	<90 ms	<70 ms
E/A	1–2	<1	1–1.5	>2
DT E	150–220 ms	>240 ms	160–220 ms	<160
PDPP	S > D	S > D	S < D	S < D
E′ mitral	8–10 $cm.s^{-1}$	E′ < A′	<8 $cm.s^{-1}$	<8 $cm.s^{-1}$

DT E, deceleration time of mitral E wave; E/A, mitral E wave and mitral A wave ratio; E′ mitral, tissue Doppler velocity in mitral annulus; PDPP, pulsed Doppler in pulmonary vein; IVRT, isovolumetric relaxation time.

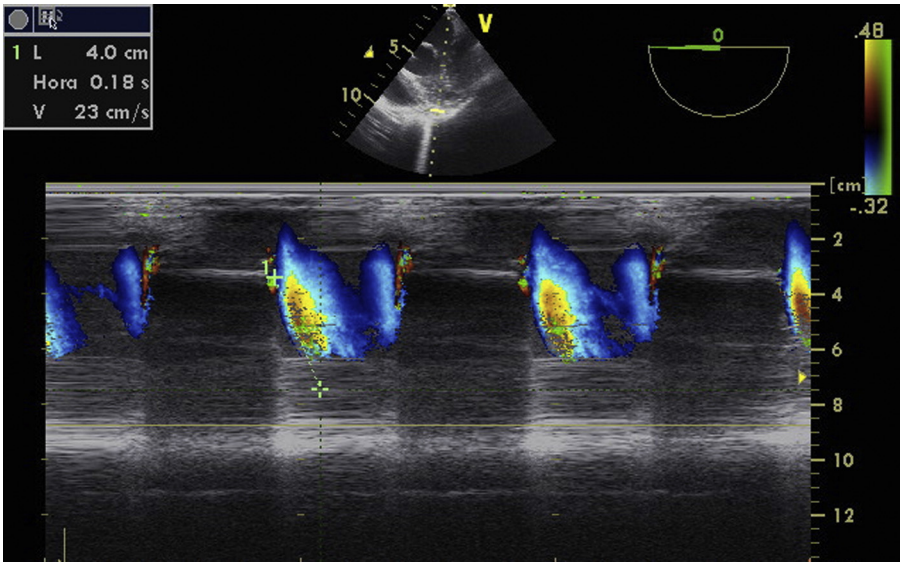

Figure 36 Color M-mode Doppler in diastolic evaluation.

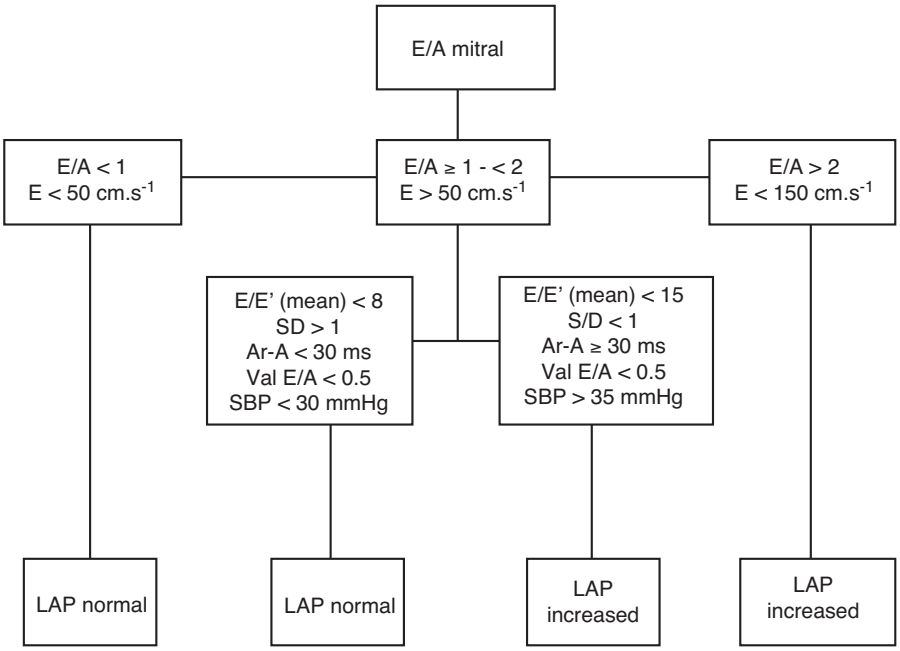

Figure 37 Flowchart of diastolic dysfunction evaluation with impaired left ventricular systolic function. E/A, mitral E wave and A wave ratio; E/E′, mitral E wave and tissue E′ wave velocity ratio; S/D, pulmonary vein systolic and diastolic ratio; Ar, reverse pulmonary A wave; LAP, left atrial pressure.

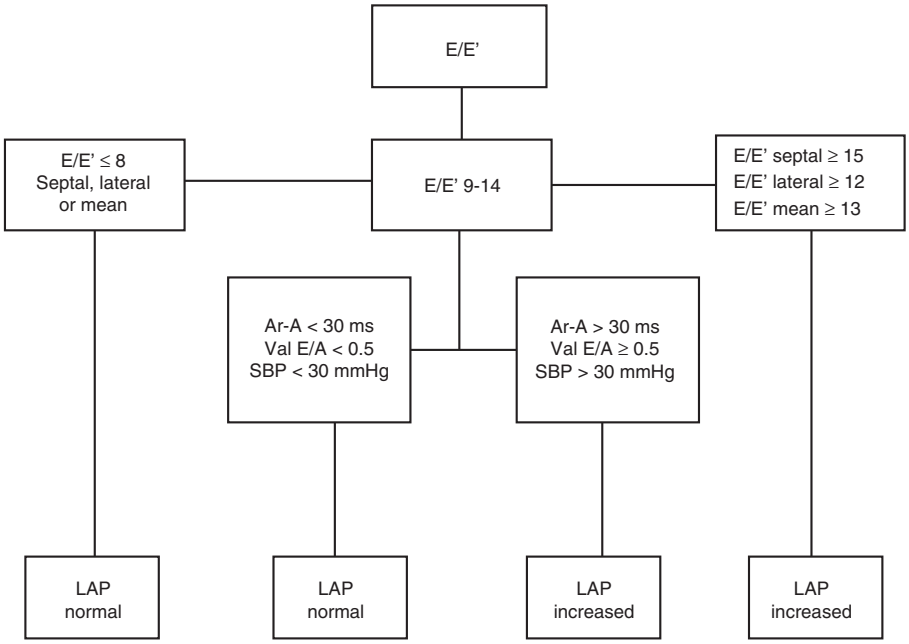

Figure 38 Flowchart of diastolic dysfunction evaluation with normal left ventricular systolic function. E/E′, mitral E wave and tissue E′ wave velocity ratio; Ar, reverse pulmonary A wave; LAP, left atrial pressure.

well as the assessment of deceleration time. Several atrioventricular blockades can lead to different atrial filling waves and also to mitral regurgitation in beats without conduction.[79] In cases of flutter and atrial fibrillation, A wave is non-existent, but deceleration time correlates well with left ventricular filling when systolic function is depressed. In these cases, E wave evaluation is also feasible and presents the same cut-off values of patients with sinus rhythm.[78]

Regarding myocardial ischemia, mitral annular tissue Doppler has been used as a reliable and early marker. Reduction of E′ wave velocity and E′/A ratio, which precede abnormalities in myocardial segmental motion, is observed.[79]

Perioperatively, multiple factors can alter and decompensate diastolic function. As seen so far, tachycardia and arrhythmia, which occur in hypovolemia and anemia, and hydroelectrolytic changes may hinder left ventricular filling. Myocardial ischemia changes calcium output from cytosol and the decoupling of actin–myosin bridges, which leads to worse LV relaxation. Increased preload, afterload, myocardial wall tension, and non-synchronous contraction lead to late and incomplete relaxation.[79]

In this scenario, Matyal et al.[79] suggest that the perioperative evaluation of diastolic function should be different in patients with impaired systolic function and normal systolic function. In patients with impaired systolic function, the assessment of diastolic function should begin with analysis of mitral E/A ratio (Fig. 37) and, in patients with preserved systolic function, diastolic evaluation should begin with the analysis of E/E1′ ratio (Fig. 38).

From the diagnosis of diastolic dysfunction and severity classification, hemodynamic targets can be established. Although future studies are required to confirm the exact accuracy of the therapeutic strategies used, it may be suggested that in patients with altered relaxation, increased left atrial pressure, and frequency control (preferably bradycardia) lead to improved ventricular filling, as they increase the pressure gradient between LA and LV, in addition to increase the filling time.[79] In patients with altered compliance, water restriction and even judicious use of diuretics, in addition to an increased blood pressure to improve coronary perfusion pressure, may be appropriate choices.[78]

Conflicts of interest

The authors declare no conflicts of interest.

References

1. Hahn RT, Abraham T, Adams MS, et al. Guidelines for performing a comprehensive transesophageal echocardiographic examination: recommendations from the American Society of Echocardiography and the Society of Cardiovascular Anesthesiologists. J Am Soc Echocardiogr. 2013;26:921–64.
2. Shanewise JS, Cheung AT, Aronson S, et al. ASE/SCA Guidelines for performing a comprehensive intraoperative multiplane transesophageal echocardiography examination: recommendations of the American Society of Echocardiography Council for Intraoperative Echocardiography and the Society of Cardiovascular Anesthesiologists task force for certification in perioperative transesophageal echocardiography. Anesth Analg. 1999;12:884–900.
3. Barbosa MM, Nunes MCP, Campos Filho O, et al. Sociedade Brasileira de Cardiologia. Diretrizes das indicações da ecocardiografia. Arq Bras Cardiol. 2009;93:e265–302.
4. Salgado-Filho MF. Diretrizes da ecocardiografia intraoperatória no Brasil. Chegou a hora de uma força-tarefa? Rev Bras Anestesiol. 2017;67:318–20.
5. Rengasamy S, Subramaniam B. Basic physics of transesophageal echocardiography. Int Anesthesiol Clin. 2008;46:11–29.
6. Galhardo Júnior C, Botelho ESL, Diego LAS. Intraoperative monitoring with transesophageal echocardiography in cardiac surgery. Rev Bras Anestesiol. 2011;61:495–512.
7. Bulwer BE, Shernan SK, Thomas JD. Physics of echocardiography. In: Savage RM, Aronson S, Shernan SK, editors. Comprehensive textbook of perioperative transesophageal echocardiography. 2nd ed. Lippincott Williams & Wilkins; 2011. p. 3–41.
8. Silva F, Arruda R, Nobre Â, et al. Impacto da ecocardiografia transesofágica intraoperatória na cirurgia cardíaca. Análise retrospectiva duma série de 850 exames. Rev Port Cardiol. 2010;29:1363–82.
9. Porter TR, Shillcutt SK, Adams MS, et al. Guidelines for the use of echocardiography as a monitor for therapeutic intervention in adults: a report from the American Society of Echocardiography. J Am Soc Echocardiogr. 2015;28:40–56.
10. Carpentier AF, Lessana A, Relland JY, et al. The ''physio-ring'': an advanced concept in mitral valve annuloplasty. Ann Thorac Surg. 1995;60:1177–85.
11. Koch CG. Assessment of the mitral valve. In: Savage R, Aronson S, Shernan SK, Shaw A, editors. Comprehensive textbook of perioperative echocardiography. 2nd ed. Wolters Kluwer/Lippincott Williams & Wilkins; 2011.
12. Dal-bianco JP, Levine RA. Anatomy of the mitral valve apparatus Role of 2D and 3D echocardiography. Cardiol Clin. 2013;31:151–64.
13. Sidebotham DA, Allen SJ, Gerber IL, et al. Intraoperative transesophageal echocardiography for surgical repair of mitral regurgitation. J Am Soc Echocardiogr. 2014;27:345–66.
14. Gething MA. Mitral valve repair: an echocardiographic review: Part 1. J Cardiothorac Vasc Anesth. 2015;29:156–77.
15. Cahalan MK, Stewart W, Pearlman A, et al. American Society of Echocardiography and Society of Cardiovascular Anesthesiologists task force guidelines for training in perioperative echocardiography. J Am Soc Echocardiogr. 2002;15:647–52.
16. Mahmood F, Hess PE, Matyal R, et al. Echocardiographic anatomy of the mitral valve: a critical appraisal of 2-dimensional imaging protocols with a 3-dimensional perspective. J Cardiothorac Vasc Anesth. 2012;26:777–84.
17. Vegas A, Meineri M, Jerath A. Real-time three-dimensional transesophageal echocardiography. A step-by-step guide. New York: Springer; 2012.
18. Andrawes MN, Feinman JW. 3-Dimensional echocardiography and its role in preoperative mitral valve evaluation. Cardiol Clin. 2013;31:271–85.
19. Shah PM, Raney AA. Echocardiography in mitral regurgitation with relevance to valve surgery. J Am Soc Echocardiogr. 2011;24:1086–91.
20. Maslow AD, Regan MM, Haering JM, et al. Echocardiographic predictors of left ventricular outflow tract obstruction and systolic anterior motion of the mitral valve after mitral valve reconstruction for myxomatous valve disease. J Am Coll Cardiol. 1999;34:2096–104.
21. Maslow A, Mahmood F, Poppas A, et al. Three-dimensional echocardiographic assessment of the repaired mitral valve. J Cardiothorac Vasc Anesth. 2014;28:11–7.
22. Maslow A. Mitral valve repair: an echocardiographic review: Part 2. J Cardiothorac Vasc Anesth. 2015;29:439–71.
23. Kim H, Bergman R, Matyal R, et al. Three-dimensional echocardiography and en face views of the aortic valve: technical communication. J Cardiothorac Vasc Anesth. 2013;27:376–80.
24. Piazza N, de Jaegere P, Schultz C, et al. Anatomy of the aortic valvar complex and its implications for transcatheter implantation of the aortic valve. Circ Cardiovasc Interv. 2008;1:74–81.
25. Doddamani S, Bello R, Friedman MA, et al. Demonstration of left ventricular outflow tract eccentricity by real time 3D echocardiography: implications for the determination of aortic valve area. Echocardiography. 2007;24:860–6.
26. Gaspar T, Adawi S, Sachner R, et al. Three-dimensional imaging of the left ventricular outflow tract: impact on aortic valve area estimation by the continuity equation. J Am Soc Echocardiogr. 2012;25:749–57.
27. Skubas N, Perrino A. Assessment of perioperative hemodynamics. In: Savage RM, Aronson S, Shernan SK, editors.

Comprehensive textbook of perioperative transesophageal echocardiography. 2nd ed. Lippincott Williams & Wilkins; 2011. p. 406–25.
28. Quiñones MA, Otto CM, Stoddard M, et al. Recommendations for quantification of Doppler echocardiography: a report from the Doppler quantification task force of the Nomenclature and Standards Committee of the American Society of Echocardiography. J Am Soc Echocardiogr. 2002;15:167–84.
29. Baumgartner H, Hung J, Bermejo J, et al. Echocardiographic assessment of valve stenosis: EAE/ASE recommendations for clinical practice. J Am Soc Echocardiogr. 2009;22:1–23.
30. Lang RM, Bierig M, Devereux RB, et al. Recommendations for chamber quantification: a report from the American Society of Echocardiography's Guidelines and Standards Committee and the Chamber Quantification Writing Group, developed in conjunction with the European Association of Echocardiography, a branch of the European Society of Cardiology. J Am Soc Echocardiogr. 2005;18:1440–63.
31. Roman MJ, Devereux RB, Kramer-Fox R, et al. Two-dimensional echocardiographic aortic root dimensions in normal children and adults. Am J Cardiol. 1989;64:507–12.
32. Vriz O, Aboyans V, D'Andrea A, et al. Normal values of aortic root dimensions in healthy adults. Am J Cardiol. 2014;114: 921–7.
33. Bandyopadhyay S, Kumar Das R, Paul A, et al. A transesophageal echocardiography technique to locate the kidney and monitor renal perfusion. Anesth Analg. 2013;116:549–54.
34. St John Sutton MG, Maniet AR, Blaivas J, et al. Atlas of multiplane transesophageal echocardiography. New York: Martin Dunitz; 2003. p. 333–468.
35. Ito A, Sugioka K, Matsumura Y, et al. Rapid and accurate assessment of aortic arch atherosclerosis using simultaneous multi-plane imaging by transesophageal echocardiography. Ultrasound Med Biol. 2013;39:1337–42.
36. Lang RM, Badano LP, Tsang W, et al. EAE/ASE recommendations for image acquisition and display using three-dimensional echocardiography. J Am Soc Echocardiogr. 2012;25:3–46.
37. Mahmood F, Jeganathan J, Saraf R, et al. A practical approach to an intraoperative three-dimensional transesophageal echocardiography examination. J Cardiothorac Vasc Anesth. 2016;30:470–90.
38. Fischer GW, Salgoi S, Adams DH. Real-time three-dimensional transesophageal echocardiography: the matrix revolution. J Cardiothorac Vasc Anesth. 2008;22:904–12.
39. Hung J, Lang R, Flachskampf F, et al. 3D echocardiography: a review of the current status and future directions. J Am Soc Echocardiogr. 2007;20:213–33.
40. Kronzon I, Tunick PA. Aortic atherosclerotic disease and stroke. Circulation. 2006;114:63–75.
41. Guidoux C, Mazighi M, Lavallée P, et al. Aortic arch atheroma in transient ischemic attack patients. Atherosclerosis. 2013;231:124–8.
42. Kurra V, Lieber ML, Sola S, et al. Extent of thoracic aortic atheroma burden and long-term mortality after cardiothoracic surgery: a computed tomography study. JACC Cardiovasc Imaging. 2010;3:1020–9.
43. Weissler-Snir A, Greenberg G, Shapira Y, et al. Transoesophageal echocardiography of aortic atherosclerosis: the additive value of three-dimensional over two-dimensional imaging. Eur Heart J Cardiovasc Imaging. 2015;16:389–94.
44. Evangelista A, Aguilar R, Cuellar H, et al. Usefulness of real-time three-dimensional transoesophageal echocardiography in the assessment of chronic aortic dissection. Eur J Echocardiogr. 2011;12:272–7.
45. Catena E, Rossi G, Ferri L, et al. Three-dimensional intraoperative echographic monitoring for endovascular stent-graft repair in a patient with type B aortic dissection. J Cardiovasc Med. 2012;13:143–7.
46. Zahn R, Gerckens U, Linke A, et al. Predictors of one-year mortality after transcatheter aortic valve implantation for severe symptomatic aortic stenosis. Am J Cardiol. 2013;112:272–9.
47. Kodali SK, Williams MR, Smith CR, et al. Two-year outcomes after transcatheter or surgical aortic-valve replacement. N Engl J Med. 2012;366:1686–95.
48. Otani K, Takeuchi M, Kaku K, et al. Assessment of the aortic root using real-time 3D transesophageal echocardiography. Circulation. 2010;74:2649–57.
49. Dwarakanath S, Castresana MR, Behr AY, et al. The feasibility of simultaneous orthogonal plane imaging with tilt for short-axis evaluation of the pulmonic valve by transesophageal echocardiography. Anesth Analg. 2015;121:624–9.
50. Filho MFS, Siciliano A, Diego LA, et al. Transesophageal echocardiography in Ross procedure. Rev Bras Anestesiol. 2011;61:344–50.
51. Ho SY, Mccarthy KP, Faletra FF. Anatomy of the left atrium for interventional echocardiography. Eur J Echocardiogr. 2011;12:11–5.
52. Ho SY, Angel CJ, Sanchez-quintana D. Left atrial anatomy revisited. Circ Arrhythm Electrophysiol. 2012;5:220–364.
53. Wa M. Heart and coronary arteries. Berlin: Springer-Verlag; 1975. p. 58–9.
54. Cartwright BL, Jackson A, Cooper J. Intraoperative pulmonary vein examination by transesophageal echocardiography: an anatomic update and review of utility. J Cardiothorac Vasc Anesth. 2013;27:111–20.
55. Blume GG, Mcleod CJ, Barnes ME, et al. Left atrial function: physiology, assessment, and clinical implications. Eur J Echocardiogr. 2011;12:421–30.
56. Pagel PS, Kehl F, Gare M, et al. Mechanical function of the left atrium – new insights based on analysis of pressure-volume relations and Doppler echocardiography. Anesthesiology. 2003;98:975–94.
57. Thomas l, Levett K, Boyd A, et al. Compensatory changes in atrial volumes with normal aging: is atrial enlargement inevitable? JACC. 2002;40:1630–5.
58. Benjamin EJ, Dagostino RB, Belanger AJ, et al. Left atrial size and the risk of stroke and death – the Framingham Heart Study. Circulation. 1995;92:835–41.
59. Manning WJ, Weintraub RM, Waksmonski CA, et al. Accuracy of transesophageal echocardiography for identifying left atrial thrombi – a prospective, intraoperative study. Ann Intern Med. 1995;123:817–25.
60. Block M, Hourigan L, Bellows WH, et al. Comparison of left atrial dimensions by transesophageal and transthoracic echocardiography. J Am Soc Echocardiogr. 2002;15:143–9.
61. Castello R, Pearson AC, Fagan L, et al. Spontaneous echocardiographic contrast in the descending aorta. Am Heart J. 1990;120:915–9.
62. Anderson DC, Halperin JL, Hart RG, et al. Patients with nonvalvular atrial fibrillation at low risk of stroke during treatment with aspirin – stroke prevention in atrial fibrillation III study. JAMA. 1998;279:1273–7.
63. Vegas A. Doppler and hemodynamics perioperative two-dimensional transesophageal echocardiography. Springer Science Business Media; 2012. p. 42–3.
64. Burch TM, Mizuguchi KA, DiNardo JA. Echo didactics: echocardiographic assessment of atrial septal defects. Anesth Analg. 2012;115:776–8.
65. Johansson MC, Eriksson P, Dellborg M. The significance of patent foramen ovale. A current review of associated conditions and treatment. Int J Cardiol. 2009;134:17–24.
66. Mertens L, Friedberg MK. The gold standard for noninvasive imaging in congenital heart disease: echocardiography. Curr Opin Cardiol. 2009;24:19–24.
67. Filho MFS, Guimaraes MNC, Campos IM, et al. Intraoperative transesophageal echocardiography to evaluate pediatric

patients undergoing atrial septal defect procedure. J Cardiovasc Dis Diagn. 2015;3:1–3.
68. Curtis JP, Sokol SI, Wang Y, et al. The association of the left ventricular ejection fraction, mortality, and cause of death in stable outpatients with heart failure. JACC. 2003;42:736–42.
69. Skiles JA, Griffin BP. Transesophageal echocardiographic (TEE) evaluation of ventricular function. Cardiol Clin. 2000;18:681–97.
70. Lang RM, Badano LP, Tsang W, et al. EAE/ASE recommendations for acquisition and display using three-dimensional echocardiography. J Am Soc Echocardiogr. 2012;25:3–46.
71. Mor-avi V, Lang RM, Badano LP, et al. Current and evolving echocardiographic techniques for the quantitative evaluation of cardiac mechanics: ASE/EAE consensus statement on methodology and indications endorsed by the Japanese Society of Echocardiography. J Am Soc Echocardiogr. 2011;24: 277–313.
72. Nikitin NP, Constantin C, Loh PH, et al. New generation 3-dimensional echocardiography for left ventricular volumetric and functional measurements: comparison with cardiac magnetic resonance. Eur J Echocardiogr. 2006;7:365–72.
73. Meris A, Santambrogio L, Casso G, et al. Intraoperative three-dimensional versus two-dimensional echocardiography for left ventricular assessment. Anesth Analg. 2014;118:711–20.
74. Hope MD, de la Pena E, Yang PC, et al. A visual approach for the accurate determination of echocardiographic left ventricular ejection fraction by medical students. J Am Soc Echocardiogr. 2003;16:824–31.
75. Yeo TC, Dujardin KS, Tei C, et al. Value of a Doppler-derived index combining systolic and diastolic time intervals in predicting outcome in primary pulmonary hypertension. Am J Cardiol. 1998;81:1157–61.
76. Filho MFS, Barral M, Barrucand L, et al. A randomized blinded study of the left ventricular myocardial performance index comparing epinephrine to levosimendan following cardiopulmonary bypass. PLOS ONE. 2015;14:e014331.
77. Odell DH, Cahalan MK. Assessment of left ventricular global and segmental systolic function with transesophageal echocardiography. Anesthesiol Clin. 2006;24:755–62.
78. Feigenbaum H, Armstrong W, Ryan T. Evaluation of systolic and diastolic function of the left ventricle, Feigenbaum's echocardiography. 6th ed. Williams & Wilkins; 2005. p. 139–80.
79. Matyal R, Skubas NJ, Shernan SK, et al. Perioperative assessment of diastolic dysfunction. Anesth Analg. 2011;113:449–72.
80. Nicoara A, Whitener G, Swaminathan M. Perioperative diastolic dysfunction: a comprehensive approach to assessment by transesophageal echocardiography. Semin Cardiothorac Vasc Anesth. 2014;18:218–36.
81. Maharaj R. Diastolic dysfunction and heart failure with a preserved ejection fraction: relevance in critical illness and anaesthesia. J Saudi Heart Assoc. 2012;24:99–121.
82. Lee E-H, Yun S-C, Chin J-H, et al. Prognostic implications of preoperative e/e ratio in patients with off-pump coronary artery surgery. Anesthesiology. 2012;116:326–71.
83. Shernan SK. Uma abordagem prática à avaliação ecocardiográfica da função diastólica ventricular. 2nd ed. Baltimore: Williams & Wilkins; 2010. p. 146–68.
84. Flachskampf FA, Badano L, Daniel WG, et al. Recommendations for transoesophageal echocardiography: update 2010. Eur J Echocardiogr. 2010;11:557–76.